826865
92L/05

Examination of the petro-chemistry of the Bonanza Group volcanic rocks, Lemare property, northwestern Vancouver Island, B. C.

Mike Holmes St#75412890
Geology 558 January 1993

TABLE OF CONTENTS

List of Tables

List of Figures

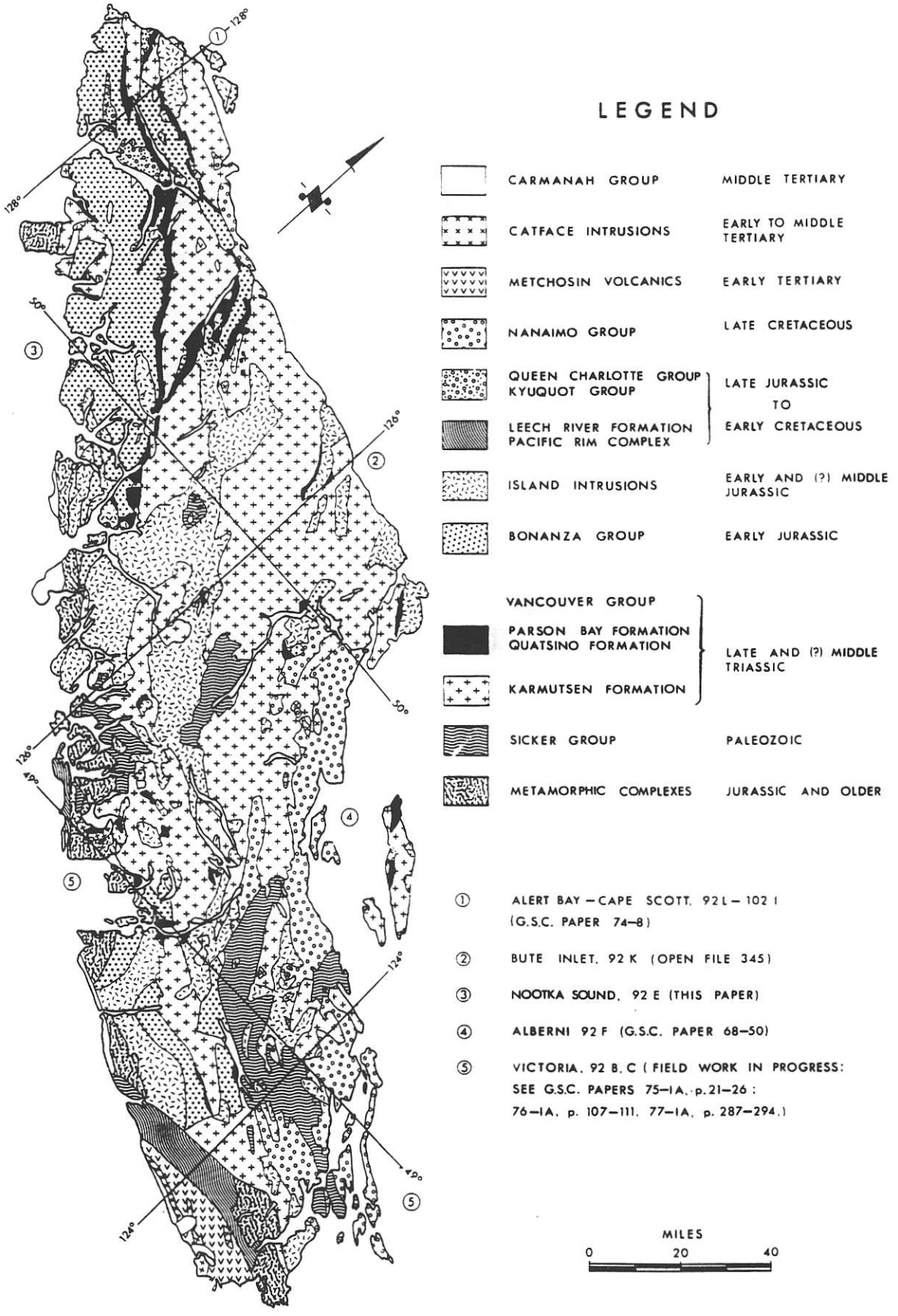

Figure 1. *Geological sketch map and index to geological mapping on Vancouver Island.* (AFTER MULLER AND NORTHCOTE, 1981)

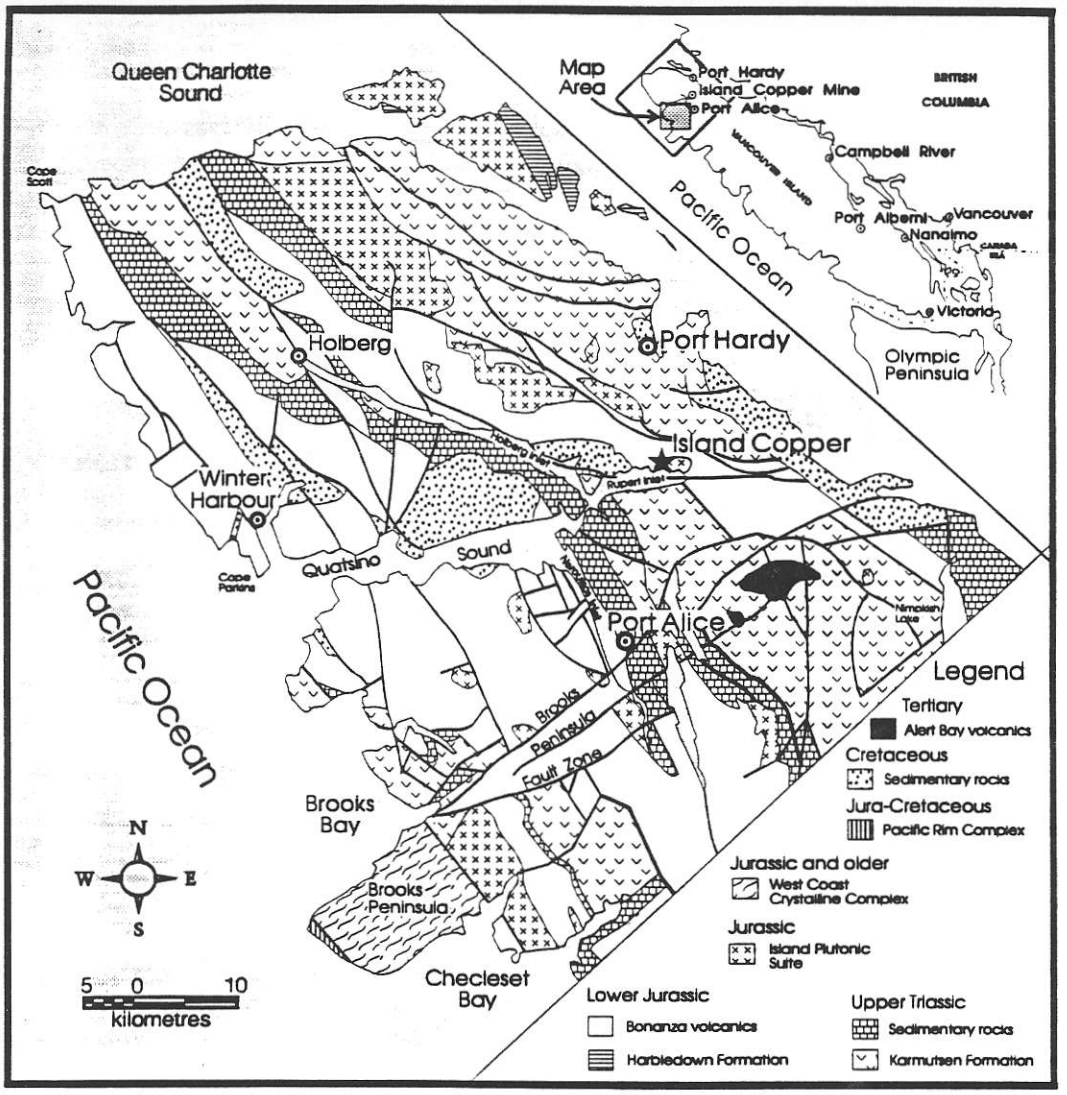

Fig. 2 Generalized geology of northern Vancouver Island (After Nixon, et al., 1993).

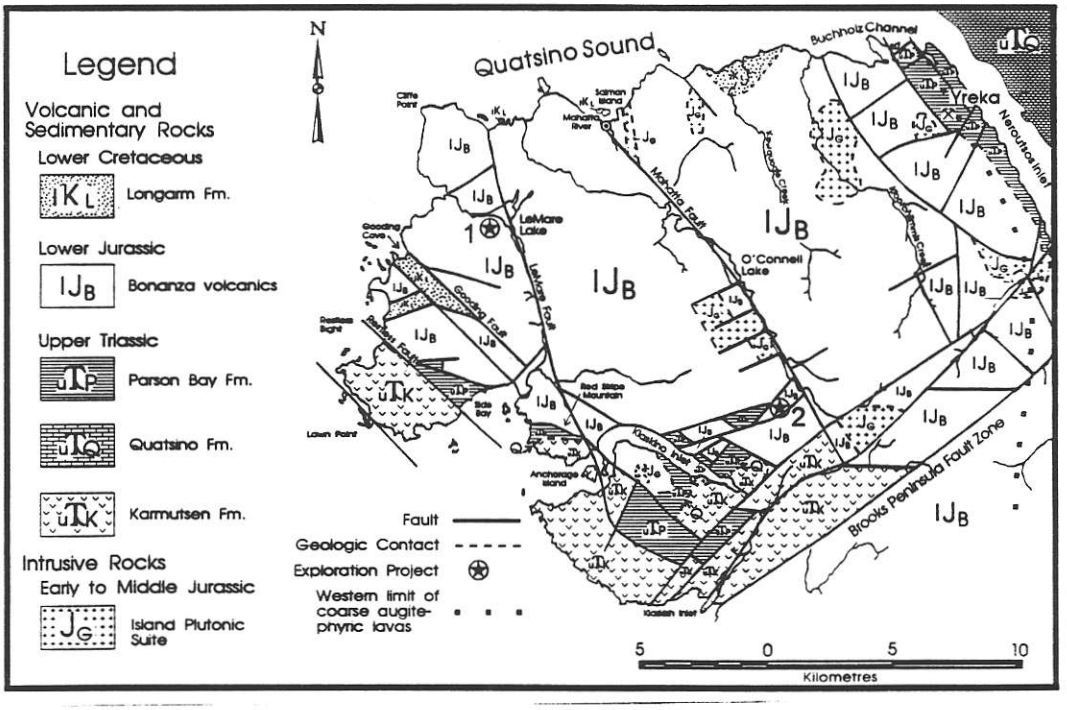

Fig. 3 General geology of Mahatta Creek area (92L/5). Q indicates the presence of Quatsino limestone at the base of the Parson Bay Formation. The star indicates an exploration project: 1, Lemare Lake, Minnova, Inc.; 2, Madhat, Pan Orvana Resources Inc. (After Nixon, et al., 1993)

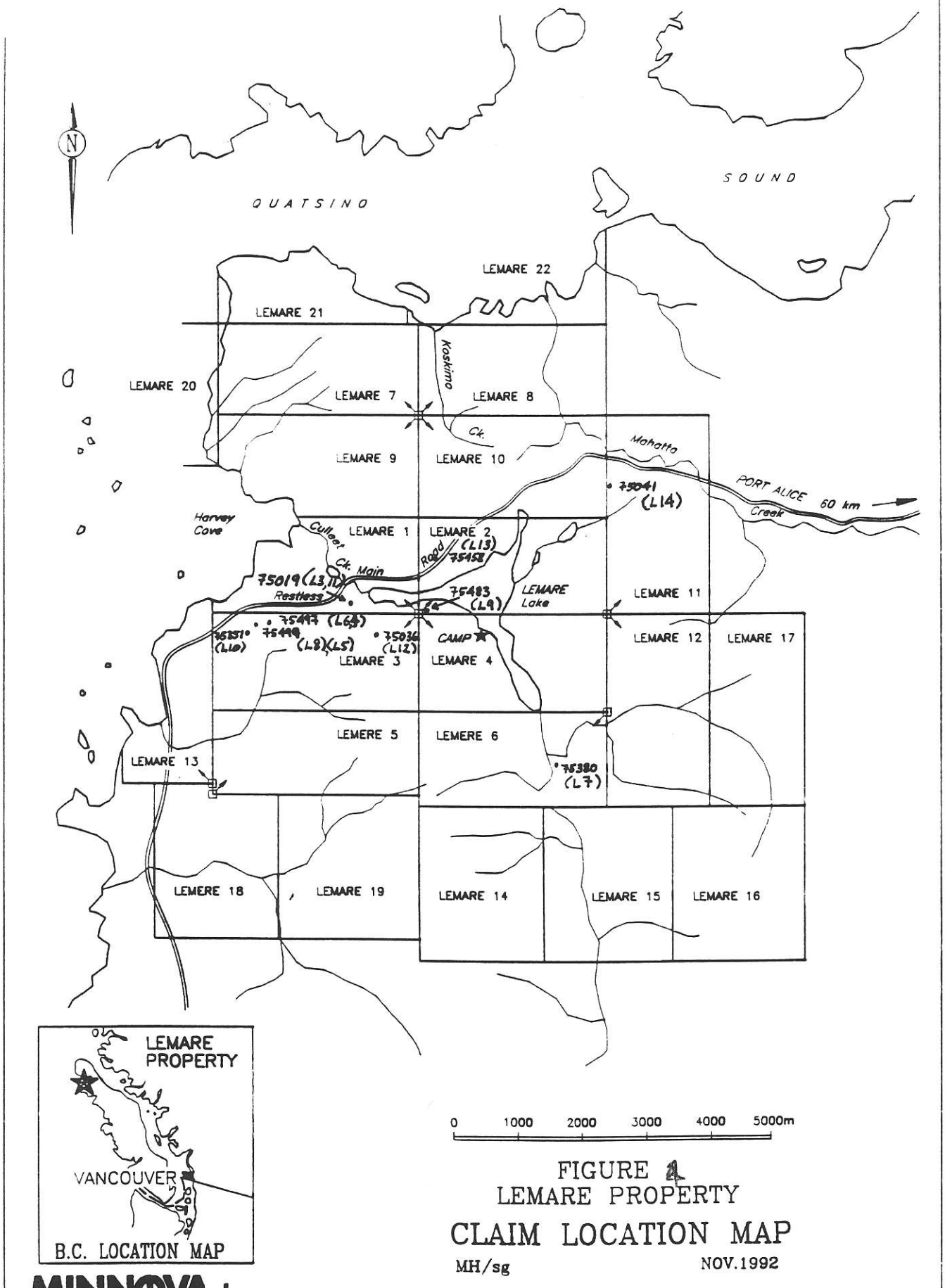

FIGURE 1
LEMARE PROPERTY
CLAIM LOCATION MAP

MH/sg NOV.1992

MINNOVA Inc.

ABSTRACT

Nine whole rock samples comprising three basalts, three andesites and three rhyolites were selected as a least altered suite of rocks from the Lemare property on northwest Vancouver Island. The nine samples were analyzed for major, minor and trace elements to provide a definitive index against which 209 whole roek samples could be compared to ascertain and corroborate the presence, type and degree of metasomatism. Pearce element analysis (PER) was used to determine: (1) whether the rock suite was comagmatic, (2) the phases involved in fractionation, and (3) the relative system sizes. An attempt is made to identify alteration related to mineralization, based on PER analysis.

1.0 INTRODUCTION

The Lemare property on northwestern Vancouver Island, British Columbia, covers an area of approximately 100 square kilometers. Less than 20 square kilometers have been mapped at a scale of 1:10 000 or larger (Fig. 4). Recconaissance by Keewatin Engineering in 1991 led to the discovery of the Gorby copper showing in the northwestern quadrant near Harvey Cove, and the South Gossan gold zone immediately west of the southern arm of Lemare Lake.

A mineral exploration program initiated in summer 1992 by Minnova, Inc. resulted in the collection of 282 whole rock samples that were analyzed by XRF. Many analyses for Y, Zr and Nb were below detection limits; these samples were precluded from this study. Thus, 209 samples were studied following the method of Pearce element ratios (PER).

2.0 REGIONAL GEOLOGY

Vancouver Island is part of Wrangellia terrane, which is in the Insular Belt of British Columbia. The main stratigraphy of the island consists of the Devonian to Permian Sicker Group basement, overlain by the Triassic Karmutsen Formation, the Triassic Quatsino and Parsons Bay Formation, and the Jurassic Bonanza Group (Figs. 1 to 3). The Bonanza Group is comagmatic with the Jurassic Island intrusions (Northcote and Muller, 1972).

Overlying this package are: the Leech River Schist, Late Mesozoic sediments, Tertiary volcanics, intrusions and sediments (Muller, 1981: Fig. 1; Nixon, et al., 1993: Figs. 2, 3). Andrew et al. (1991) found that the neodymium, strontium and lead isotope magmatic arc signatures of the Bonanza Group volcanics and the Island intrusions are compatible with mixing of magma from a depleted mantle source and crustal material of the underlying Sicker Group--rather than mixing of magma with material of continental origin. Thus the Early to Middle Jurassic Bonanza Group and Island intrusions are considered co-genetic. Andrew and Godwin (1988) found from lead and strontium isotope analyses that the Island intrusions showed a greater degree of contamination than the Bonanza volcanics. They also postulated that all or part of the mixing trend was due to the assimilation of Sicker material by the intrusions and that the volcanics and intrusions were co-genetic. Andrew et al. (1991) add the possibility that "the mixing trend could derive from a mantle lithosphere contaminated by Sicker magma--the mechanism could be either crustal assimilation, lithosphere melting and zone extraction, subduction of Sicker detritus, or most probably a combination of all these processes affecting mantle - derived magma. "

The Bonanza arc shows relatively high and uniform niodymium epsilon values, low strontium epsilon values, and generally lower 207/204 lead isotope ratios than any other calc-alkaline suite on Vancouver Island (Andrew et al., 1991). This supports the view that the Bonanza arc was more isolated from sources of continental material than the Sicker arc (Andrew and Godwin, 1988). The calc-alkaline chemistry, felsic nature, and correlation of initial strontium and lead isotope ratios strongly suggest an island arc setting.

Paleomagnetic data from Symons (1983) gives a date of 190 Ma for the Bonanza volcanics and 180 Ma for the Island intrusions. This indicates that exposed intrusions were emplaced in the waning stages of volcanism. The Bonanza Group volcanics, 2 000 to 2 500 m thick, are composed mainly of andesite to rhyolite flows, tuffs and breccias,

with minor basalt flows at the base (Northcote and Muller, 1972). The predominance of felsic pyroclastics is indicative of an extremely explosive volcanic environment.

3.0 PROPERTY GEOLOGY

The Lemare property consists of northwest to northeast striking rhyolites, intermediate volcanics and basalts that dip 20 to 40 degrees southwest to northwest. The units are gently folded and consist mainly of massive to flow banded rhyolites that are often autobrecciated. The flow banding in the rhyolites ranges from 2 to 25 mm and is demonstrably consistent in attitude over several square kilometers. Intermediate andesites, trachyandesites and rhyodacites occur mainly as fine grained tuffs with rare flows. Heterolithic clasts, homolithic clasts and welded textures are evident in the various tuffs in the northwestern part of the property. The more uncommon basalt flows are usually relatively thin (< 100 m), vessicular and sandwiched between thick rhyolite flows. A thick basalt flow in the western part of the property is flanked by intermediate pyroclastic rocks.

Numerous faults with north, east and southeast trends cut the property. Timing of, and displacement of, these faults is uncertain. The Gorby copper showing lies at the juncture of several of the southeast trending faults. A south to southeast trending fault along the valley and the southern arm of Lemare Lake may account for the different attitudes on the two sides of the arm.

The Gorby copper area is marked by porphyry style alteration. Potassic alteration of secondary, salmon-pink K-feldspar associated with magnetite, hematite, rare bornite and minor chalcopyrite characterize the showing area. Grab samples yield up to 3% copper. About 100 m from the area of the showing, propylitic alteration of calcite veins, and pervasive chlorite and epidote is apparent. A small zone of advanced argillic alteration consisting of sericite-pyrophyllite+/-kaolinite occurs adjacent to a fault about 500 m east-southeast of the Gorby showing. Occasional small shears marked by phyllic alteration, but generally less than 2 m across, dot the property. The phyllic alteration consists of quartz-

sericite-pyrite. These zones are too infrequent and too small to help define general patterns. Rare jasper occurs locally, especially as a matrix to a large homolithic auto-brecciated rhyolite flow unit that contains conspicuous silica-filled (locally sulfide filled) lithphysae.

The South Gossan zone commences 170 m above the west side of the southern arm of Lemare Lake and extends up 400 m to where it is truncated by the easternmost of the north trending faults (Fig. 4). The gossanous appearance is from abundant jarosite. The zone is characterized by pervasive epithermal-style alteration consisting of quartz-kaolinite-pyrophyllite-dickite+/-montmorillonite; causitive veining is sparse. Numerous steeply dipping mafic dykes and phyllic-altered shears (quartz-sericite-pyrite) occur over the zone.

4.0 ANALYTICAL METHODS

4.1 Background data

Whole rock samples were collected for analysis at 100 m spacing along logging roads that access the property claim units: Lemare 1 to Lemare 12 (Fig. 2). Samples were then shipped to Min-En Labs in Vancouver. Analysis was done for the ten major elements in weight percent oxide: SiO_2, Al_2O_3, Na_2O, CaO, MgO, K_2O, P_2O_5, TiO_2, MnO, Fe_2O_3. Trace and minor elements in ppm determined were: Y, Zr, Nb, Rb, Sr, Ba and Cr.

4.2 Selection of index samples

Initially, the samples were sorted by silica content into: (1) basalts: $SiO_2<53\%$, (2) andesites: $53\%<SiO_2<63\%$, and (3) rhyolites: $SiO_2>63\%$. This grouping was consistent with grouping of data on discrimination plots (Figs. 5-8) of Winchester and Floyd (1977), Cox et al. (1979), and Pearce and Cann (1973).

Nine samples were chosen as least altered rocks to provide an index against which other samples could be examined. These rocks were selected using the following criteria:

(1) those with values of SiO_2, LOI, CaO, Na_2O, K_2O and Fe_2O_3 specified in Table 1, and (2) those with the closest match to the fractionation lines depicted in: (a) Al_2O_3/Zr vs. SiO_2 (Fig. 9), (b) Al_2O_3/Zr vs. CaO (Fig. 10), and (c) Al_2O_3/Zr vs. Fe_2O_3 (Fig. 11).

Table 1: Selection criteria for least altered index samples from the Lemare property, northwestern Vancouver Island, B.C.

	SiO_2 (%)	LOI (%)	CaO (%)	Na_2O (%)	K_2O (%)	Fe_2O_3(%)
Basalts	< 53.0	< 3.5	6.0-7.5	3.5-4.5	1.0-1.3	9.5-10.5
Andesites	53.0-63.0	< 3.5	3.8-6.0	4.4-5.2	2.0-2.2	6.9-7.6
Rhyolites	> 63.0	< 2.5	0.6-1.8	1.3-4.0	4.2-6.4	3.1-5.7

4.3 Analysis of index samples

Selected index samples were sent for whole rock analysis to a different lab (XRAL, Toronto). Two Mineral Deposit Research Unit (MDRU) standards (QGRM100 and P1) and three duplicate samples were submitted with the index samples to monitor precision and accuracy. A total of 14 samples were analyzed. Comparison and precision of the MDRU standards (QGRM100and P1) is presented in Table 4. The precision of the conserved elements (TiO_2 and Zr) for the MDRU standards and the duplicates from the Lemare property is depicted graphically in Figure 12. A comparison of sample analyses between the Min-En Lab and the X-Ray Assay Lab is presented in Tables 2 and 3.

Table 2: Selected Min-En Lab sample analyses

#	LOI wt. %	SiO_2 wt. %	CaO wt. %	Fe_2O_3 wt. %	K_2O wt. %	Na_2O wt. %	P_2O_5 wt. %	Al_2O_3 wt. %	TiO_2 wt. %
75499	3.3	49.26	7.25	9.74	1.13	3.93	0.24	16.36	0.85
75380	3.4	49.05	7.59	9.93	1.20	3.75	0.24	16.08	0.96
75036	3.4	49.68	6.05	10.4	1.15	4.5	0.22	15.98	0.91
75041	3.4	55.43	4.75	6.96	2.13	5.15	0.16	15.42	0.69
75497	2.6	56.59	5.77	7.40	2.14	4.49	0.18	15.29	0.71
75351	3.3	56.59	3.87	7.58	2.16	4.90	0.28	15.48	0.82
75019	1.6	70.41	1.75	3.18	4.37	3.93	0.04	13.01	0.25
75483	2.2	69.66	1.20	5.63	5.67	1.35	0.05	12.14	0.32
75458	2.3	65.41	0.63	4.99	6.23	2.65	0.15	13.71	0.59

Table 3: Selected X-Ray Assay Lab (XRAL) sample analyses

#	LOI wt. %	SiO_2 wt. %	CaO wt. %	Fe_2O_3 wt. %	K_2O wt. %	Na_2O wt. %	P_2O_5 wt. %	Al_2O_3 wt. %	TiO_2 wt. %
75499	3.15	49.2	7.25	9.69	1.38	3.73	0.24	16.5	1.06
75380	3.25	49.2	7.48	10.2	1.06	4.14	0.24	15.8	1.15
75036	4.85	48.2	4.30	11.1	0.43	5.24	0.25	18.0	1.15
75041	4.15	54.0	4.93	7.68	2.13	4.95	0.17	15.8	0.902
75497	2.40	56.0	4.56	7.36	2.67	4.63	0.19	15.6	0.879
75351	2.95	57.1	1.77	7.47	2.61	4.77	0.31	15.7	1.05
75019	1.40	73.4	0.77	2.75	4.47	3.75	0.05	12.4	0.317
75483	1.70	71.1	0.25	5.82	5.10	1.43	0.07	11.8	0.415
75458	2.55	66.0	1.06	7.44	5.51	0.79	0.23	11.1	0.818

Table 4: X-Ray Assay Lab (XRAL) precision of standards

X	#	LOI wt. %	SiO_2 wt. %	CaO wt. %	Fe_2O_3 wt. %	K_2O wt. %	Na_2O wt. %	P_2O_5 wt. %	Al_2O_3 wt. %	TiO_2 wt. %
1	QGRM100	0.15	48.2	8.46	14.7	1.05	2.89	0.20	15.7	1.99
2	duplicate	0.35	47.8	8.34	14.6	1.04	2.85	0.20	15.5	1.99
3	**%difference**	**57**	**0.83**	**1.4**	**0.68**	**0.95**	**1.4**	**0.0**	**1.3**	**0.0**
4	MDRU-VALUE	0.27	48.6	8.48	15.2	1.01	2.81	0.19	15.35	1.98
5	**%difference**	**9.1**	**1.2**	**0.94**	**3.6**	**3.5**	**2.1**	**5.0**	**1.6**	**0.50**
6	P1	0.55	69.2	3.54	3.73	2.03	4.07	0.09	14.4	0.453
7	MDRU-VALUE	0.45	70.1	3.61	3.8	1.97	4.03	0.09	14.4	0.403
8	**%difference**	**17**	**1.2**	**1.9**	**1.8**	**3.0**	**0.98**	**0.0**	**0.0**	**11**
9	SY-2	0.0	59.5	7.96	6.16	4.43	4.40	0.43	12.2	0.186
10	duplicate	0.0	59.6	7.95	6.17	4.42	4.35	0.43	12.1	0.186
11	**%difference**	**0.0**	**0.17**	**0.13**	**0.16**	**0.23**	**1.1**	**0.0**	**0.82**	**0.0**

The MDRU values in Table 4 are an average of values taken from several labs.

In row 3: % difference = $100 - (x_1/x_2*100)$ where, x_1 and x_2 are the Xral original and duplicate values for the MDRU standard QGRM100 (i.e. rows 1 and 2).

In row 5: % difference = $100 - (x_3/x_4*100)$ where, $x_3 = (x_1+x_2)/2$, and x_4 = the MDRU value for the QGRM standard QGRM100.

In row 8: % difference = $100 - (x_6/x_7*100)$ where, x_6 = the XRAL value for the MDRU standard P1 and, x_7 = the MDRU value for the MDRU standard P1.

In row 11: % difference = $100 - (x_9/x_{10}*100)$ where, x_9 and x_{10} equal the XRAL internal standard and duplicate (SY-2).

5.0 ROCK SUITE CHARACTERIZATION

5.1 Introduction

The rocks on Lemare property fall into three general suites: basalts, intermediate volcanics and rhyolites. The basalts are generally dark grey to black, medium to fine grained, vessicular and massive. They often contain calcite as veins and amygdals. The rhyolites are readily distinguishable. They are moderate grey to green, very fine grained to glassy, massive to brecciated, often with thin lamellar flowbanding (2 - 25 mm); in the Gorby area they contain abundant silica-filled (+/-sulfide) lithophysae. The intermediate volcanics tend to be more difficult to distinguish. They range in colour and texture between that of the basalts and the rhyolites.

5.2 Classification

In a volcanic discrimination plot (Fig. 5) of log (Zr/TiO_2) vs. log (Nb/Y) , Lemare basalts plot mainly in the alkaline-basalt field, while in an oceanic discrimination plot (Fig. 6) of Zr vs. Ti they plot as calc-alkaline basalts. The intermediate volcanics plot (Fig. 7) mainly in the trachyandesite to andesite to rhyodacite/dacite field in a log (Zr/TiO_2) vs. log (Nb/Y) plot; a few samples plot in the basalt/andesite/rhyolite fields. In a separate plot, but with the same axes (Fig. 8), rhyolites cluster in the rhyolite and rhyodacite/dacite fields; a few samples plot in the trachyandesite field.

5.3.0 Pearce element ratios (PER)

The use of Pearce element ratios (PER) requires (Madeisky and Stanley, 1992): (1) an initially homogeneous system, (2) the presence of at least one conserved constituent, and (3) a material transfer process, such as metasomatism. Molar concentration units are used instead of mass concentration units because: (1) they relate directly to mineral formulae and chemical reactions, (2) solid solution mineral composition variations can be accommodated through simple addition, and (3) the coefficients for soluble species in metasomatic reactions can be calculated through simple subtraction. Ti, Zr and Y

commonly are incompatible elements in calc-alkaline rocks. These elements were examined in scatterplots--along with Nb, Ti and P--to ascertain the conserved constituents. P, Nb and Y exhibited some mobility, and thus, Zr and Ti were selected. Ti may experience some compatibility due to the crystallization of minor Fe-Ti oxides. Therefore Zr was chosen as the favoured PER conserved constituent, and is used as the denominator of ratios in presented PER diagrams.

5.3.1 PER: XRAL (index) data

The scatterplot in Figure 12 depicts three distinct differentiation trends of the basalts, intermediate volcanics and rhyolites. Apparent cogeneity is observed for the basalts and for the rhyolites. However, the intermediate volcanics do not define a straight line through the origin. They therefore do not appear to be co-magmatic. One of the rhyolite samples (#MHL-13 = 75458) exhibited an anomalous signature and is discarded from further consideration.

A PER diagram of Ti/Zr vs. P/Zr for all XRAL data (Fig. 13) corroborates the subdivision of the Bonanza Group volcanics into three suites. The same PER diagram applied to the basalts only (Fig. 14) shows all the basalts to be co-magmatic. When the basalts are plotted on a 'Q' plot, [which accounts for plagioclase, olivine, pyroxene and Fe-oxide fractionation (Nicholls and Russell, 1991; Fig. 15], they show a high correlation coefficient (R2) of 0.995 falling on an average slope of 1.07. [A slope of 1.00 accounts perfectly for fractionation of the depicted phases, and an R2 of 1.00 means that the data fall exactly on that line (Nicholls and Russell, 1991).] The Intermediate volcanics in Figure 17 show a lower R2 of 0.852 falling on a slope of -0.412. This indicates that one of the two, but not both, are involved in fractionation along with plagioclase. [A slope of -1.00 would mean that plagioclase fractionation alone was involved (Nicholls and Russell, 1991).] A much better fit (m = 1.02, R2 = 0.975) is observed in the PER diagram for intermediate volcanics that accounts for the fractionation of plagioclase and pyroxene

(Fig. 16). No fractionation plots attempted for the rhyolites attained useful slopes near to 1.00 (Table 2).

5.3.2 PER: Lemare basalt

Lemare basalts plot within the calc-alkaline field (Fig. 4) and appear to be comagmatic on the PER diagram of Ti/Zr vs. P/Zr (Fig. 18). A PER diagram accounting for plagioclase fractionation (Fig. 19) exhibits a good slope (m = 1.07), but a poor correlation coefficient (R2 = 0.366). In Figure 20 a fixed slope of unity was drawn through one of the index samples (75380) to examine whether the alteration reflects depletion or addition by calclum and sodium. It is evident that the fixed slope is very similar to the average slope with exactly the same correlation coefficient. This indicates that the metasomatism involved is due equally to addition and subtraction of calcium and sodium. This is in agreement with the extensive propylitic (addition of Ca and Na) and potassic (subtraction of Ca and Na) alteration in different parts of the property. The 0.06 difference in Y-slope intercept (i.e. initial composition) between the fixed and average axes plots is within expected error. The scatter is reduced, with a greatly improved correlation coefficient (R2 = 0.935), when fractionation of olivine, pyroxene and Fe-oxides are accounted for along with plagioclase in a 'Q' plot (Fig. 21). The average axis (m = 0.952) for this plot has the same correlation coefficient (R2 = 0.935) as a 'Q' plot with a fixed slope of unity drawn through the index sample (75380 in Fig. 22). The Y-slope intercept difference (0.06) is the same as in the plagioclase fractionation plot. Because of the spatial separation along the axes the system appears to be relatively large. As indicated above, metasomatism is reflected by almost equal addition and subtraction of: Al, Fe, Mg, Ca and Na. Minor silicification and Ti crystallization (in Fe-Ti oxides) is indicated.

5.3.3 PER: Lemare intermediate volcanic rocks

The data scatter observed in the intermediate PER diagram of Ti/Zr vs. P/Zr (Fig. 23) indicates that the samples were probably from different magma batches (i.e. they are not comagmatic). This is further illustrated when plotted on a diagram accounting for alkali

fractionation (Fig. 24) where separation into at least 3 separate batches is possible. Affixing a slope of unity through the index sample (75497) allows observation of alkali addition for at least one group, and alkali depletion for the other groups. A PER diagram 'Q' plot reveals an average axis near unity (m = 1.03) with a high correlation coefficient (R2 = 0.982). This axis accounts almost perfectly for the fractionation of plagioclase, olivine, pyroxene and Fe-oxides. A fixed slope of unity through the index sample (75497) shows the same correlation coefficient and indicates that each of the batches underwent addition of the following: Al, Mg, Ca, and possibly, Si, Ti and Fe.

5.3.4 PER: Lemare rhyolite

The PER diagram of Ti/Zr vs. P/Zr (Fig. 27) indicates that the rhyolites, with one exception, are comagmatic. Affixing a slope of unity through the index sample (75019) on the PER alkali fractionation diagram of Figure 28 reveals that the majority of the rhyolites have undergone a relatively uniform, moderate degree of alkali depletion (i.e. a decrease in Na and K). Rare exceptions fall above and below the line. These are probably locally altered due to any of the numerous small shear zones that dot the property. The system is of moderate size in comparison to the basalts. Samples selected appear to be represented more by the more evolved rhyolites (i.e. a greater proportion of the samples cluster on the origin side of the system). These more evolved rhyolites are marked by an increase in alkali depletion over that of the less evolved rhyolites. This indicates that alteration and associated mineralization events may have occurred as the more evolved rhyolites were being extruded. This is corroborated in a PER felsic fractionation diagram (Fig. 29) that, although showing slightly more scatter, is similar to the alkali fractionation diagram of Figure 28.

6.0 CONCLUSION

Nine rock samples comprising three basalts, three intermediate volcanics and three rhyolites were selected from a property-wide program of 282 whole rock analyses as least altered samples according to criteria in Table 1 and Figures 9 to 11. (One of the rhyolite samples <MHL-13=75458 > was subsequently discarded due to an anomalous signature.) The chosen samples were used as a reference (as fresh rocks) against which the remaining samples were measured to ascertain: the cogeneity of magma batches, the fractionated phases within the batches, the degree and type of metasomatism (including the specific elements involved) and the size of the systems.

The three groups of rocks are not comagmatic with each other. Individually, the basalts and the rhyolites are comagmatic whereas the intermediate volcanics are not. Fractionation of the basalts included crystallization of plagioclase, olivine, pyroxene and Fe-oxides [specifically Fe_2TiO_4, although other Fe-Ti oxides may account for some data variation (Nicholls and Russell, 1991)]. Minimal silicification has occurred. Metasomatism is reflected by varying, almost equal, amounts of depletion and addition of: Al, Fe, Mg, Ca and Na. Fractionation trends indicate a relatively large system size with possibly more metasomatism occurring in more evolved intermediate volvanics.

Rhyolites are comagmatic. The random sample that falls outside of the major cluster (Fig. 27) may be due to local alteration from one of the small shear zones that dot the property. The system size is relatively small, roughly half the size of the basalt system. Significant alkali and felsic metasomatism has caused the removal of Na, K and Ca: The apparent increase in metasomatism of the more evolved rhyolites infers an increase in activity that may reflect mineralizing events. If this is true, then sulfide mineralization may be constrained to the latter half of the rhyolite eruptive sequence.

The intermediate volcanics are not comagmatic. They plot in fields indicating at least three separate magma batches (Figs. 23 to 26). The system sizes of individual magma batches appear to be relatively small, roughly half the size of the rhyolite system. The

middle batch appears to be more evolved than the remaining batches. Fractionation included plagioclase, olivine, pyroxene and Fe-oxides (Fe_2TiO_4). Metasomatism is expressed by addition of Al, Fe, Mg and Ca (Fig. 26). Specific batches show either uniform Na and K addition, or depletion (Fig. 24). The apparent non-consanguinity of these intermediate volcanics may reflect either contamination by underlying Sicker material (Andrew and Godwin, 1988), or assimilation or derivation of mantle lithosphere contaminated by Sicker material (Andrew et al., 1991), or simply isolated magma chambers.

REFERENCES

Andrew, A., Armstrong, R.L., and Runkle, D. (1991): Neodymium - Strontium - Lead isotopic study of Vancouver Island igneous rocks; in Can. Journ. of Earth Sciences, V. 28 (No. 11), pp. 1744-1752.

Andrew, A. and Godwin, C.I. (1988): Lead -and Strontium- isotope geochemistry of the Paleozoic Sicker Group and Jurassic Bonanza Group Volcanic rocks and Island intrusives, Vancouver Island; in Can. Journ. of Earth Sciences, V. 26 (No. 5), pp. 894-907.

Bates, R.L. and Jackson, J.A. (1990): GLOSSARY OF GEOLOGY. Third Edition, American Geological Institute, Alexandria, Virginia.

Currie, R.G. and Muller, J.E. (1976): Magnetic Susceptibility as a diagnostic parameter of Vancouver Island volcanic rocks. G.S.C. Paper 76-1B, Report of Activities Part B, pp. 97-98.

Madeisky, H.E. (1992): A system for the characterization of litho-geochemical alteration patterns resulting from primary dispersion of hydrothermal fluids controlling massive sulfide mineralization in volcano-sedimentary rocks. Research progress report for Hemac Exploration, Ltd. Vancouver, B.C.

Muller, J.E., Cameron, B. and Northcote, K.E. (1981): Geology and mineral deposits of Nootka Sound map area (92E) Vancouver Island, British Columbia. G.S.C. Paper 80-16.

Nicholls, J. and Russell, J.K. (1991): Major-element chemical discrimination of magma-batches in lavas from Kilauea Volcano, Hawaii, 1954-1971 eruptions. Canadian Mineralogist, V. 29, pp. 981-993.

Nixon, G.T., Hammack, J.L., Hamilton, J.V. and Jennings, H. (1993): Preliminary geology of the Mahatta Creek Area, northern Vancouver Island. In Geological Fieldwork 1992, Paper 1993-1, pp. 17-35.

Northcote, K.E. and Muller, J.E. (1972): Volcanism, plutonism and Mineralization: Vancouver Island; in CIM Bulletin 65 (No. 726), pp. 49-57.

Russell, J.K. and Nicholls, J. (1988): Analysis of petrologic hypotheses with Pearce element ratios. Contrib. Mineral. Petrol. 99: pp. 25-35.

Symas, D.T.A. (1983): Geotectonics of the Vancouver Island segment of Wrangellia from paleomagnetism of the Westcoast Complex. G.A.C., Program - with - Abstracts, V. 8, p. A67.

pg. 15 : YOLE + IRVING 83 - - - - PAPER GOT MUNGED

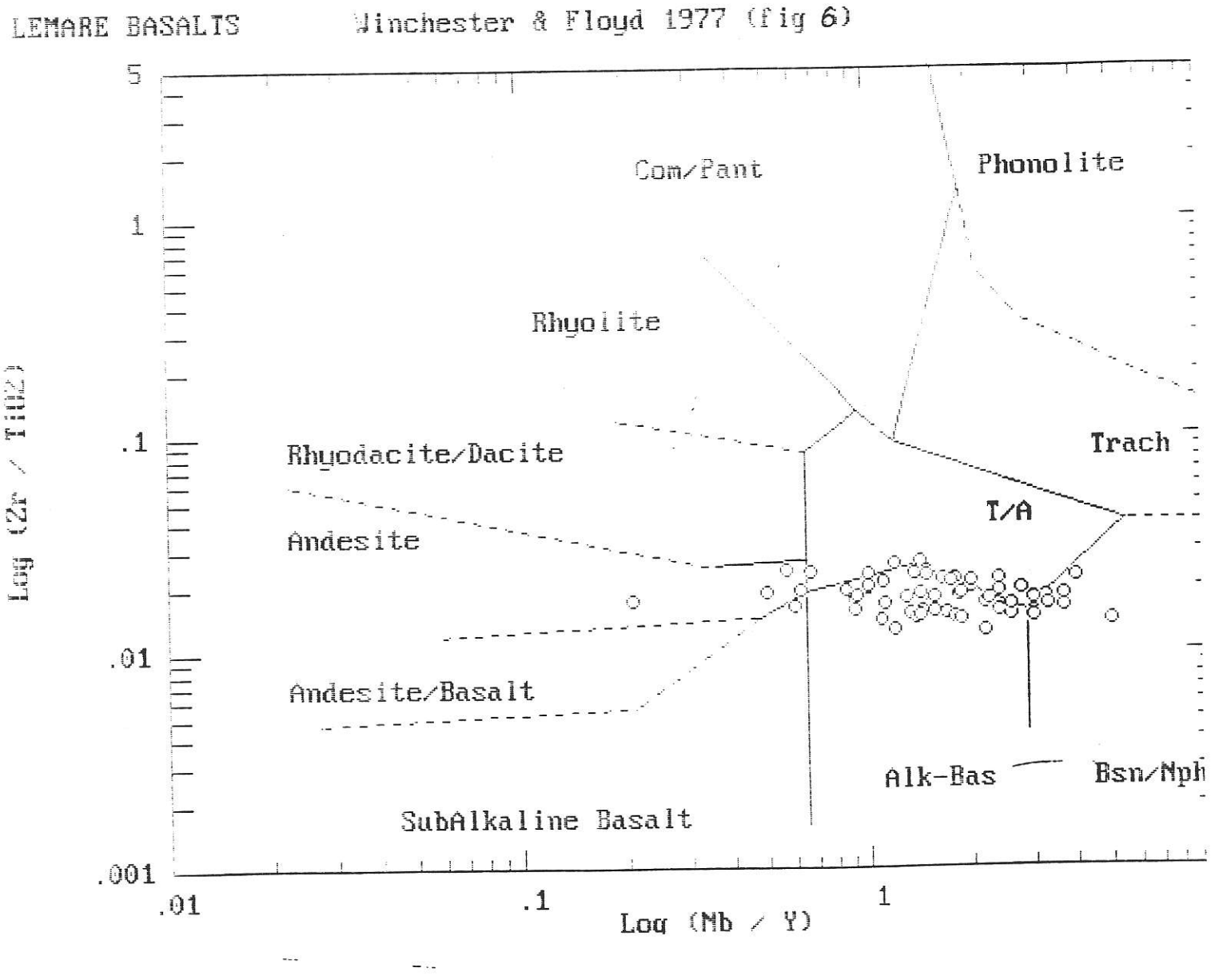

fig. 5 Discrimination plot for Lemare basalts

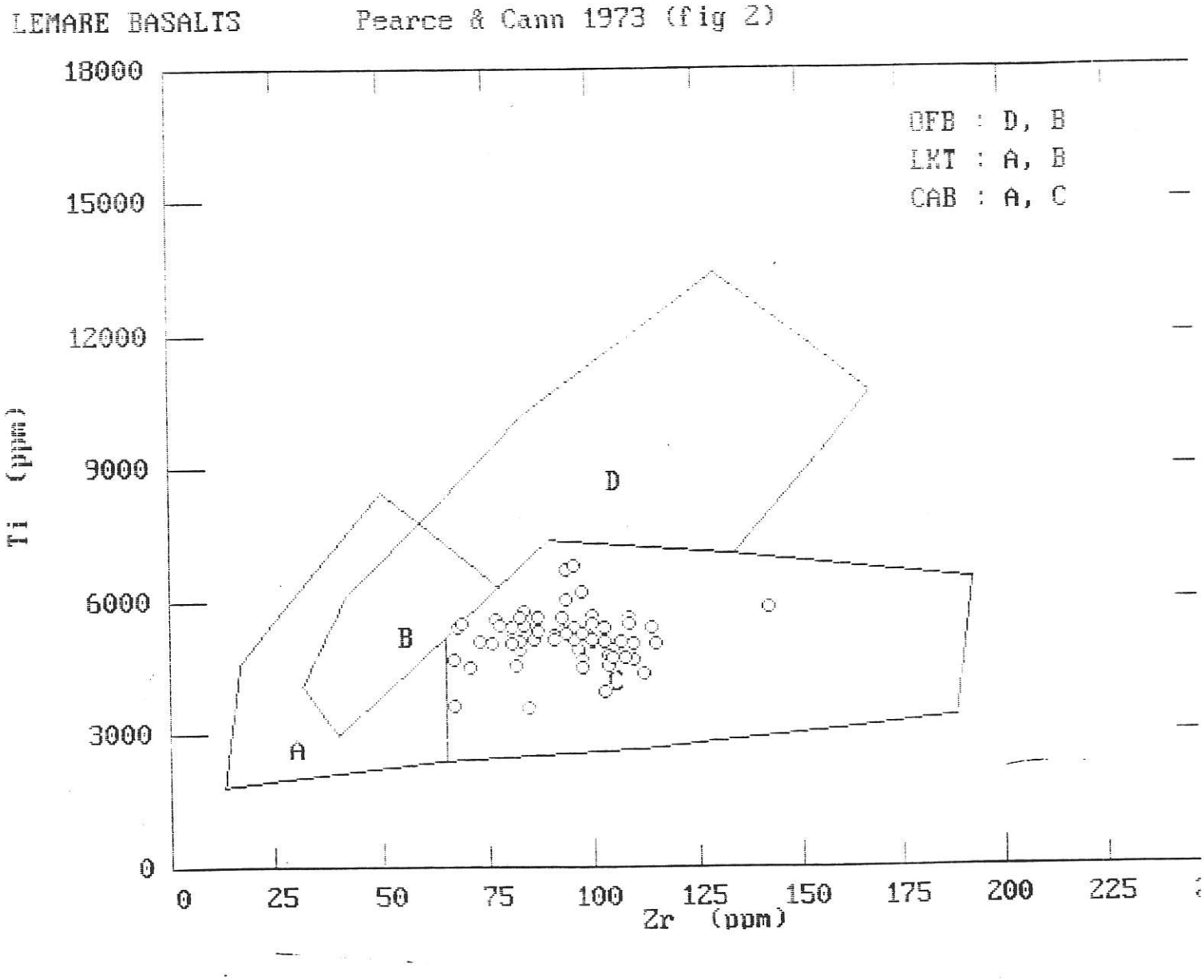

fig. 6 Tectonic setting discrimination plot for Lemare basalts

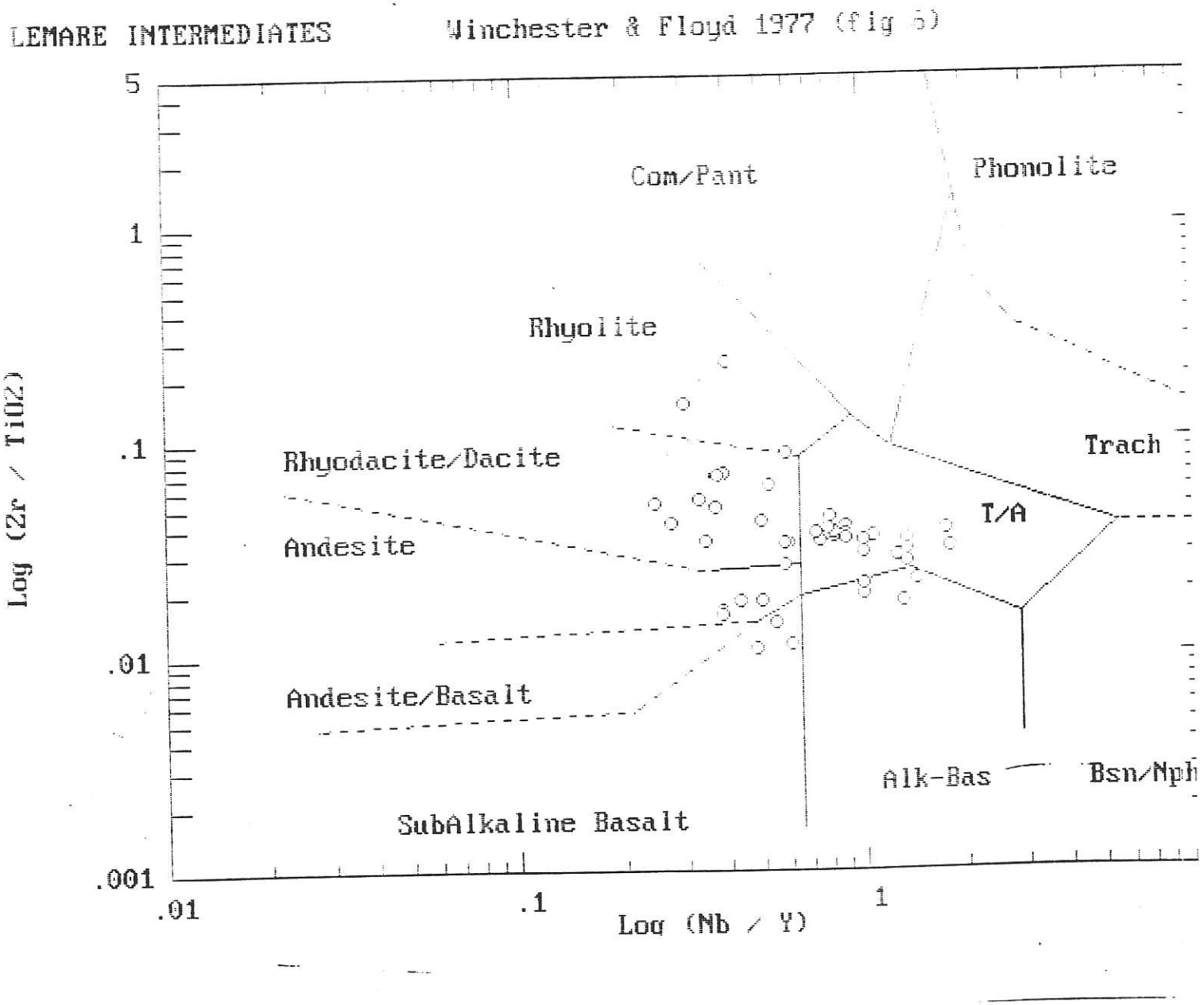

fig. 7 Discrimination plot for Lemare intermediates

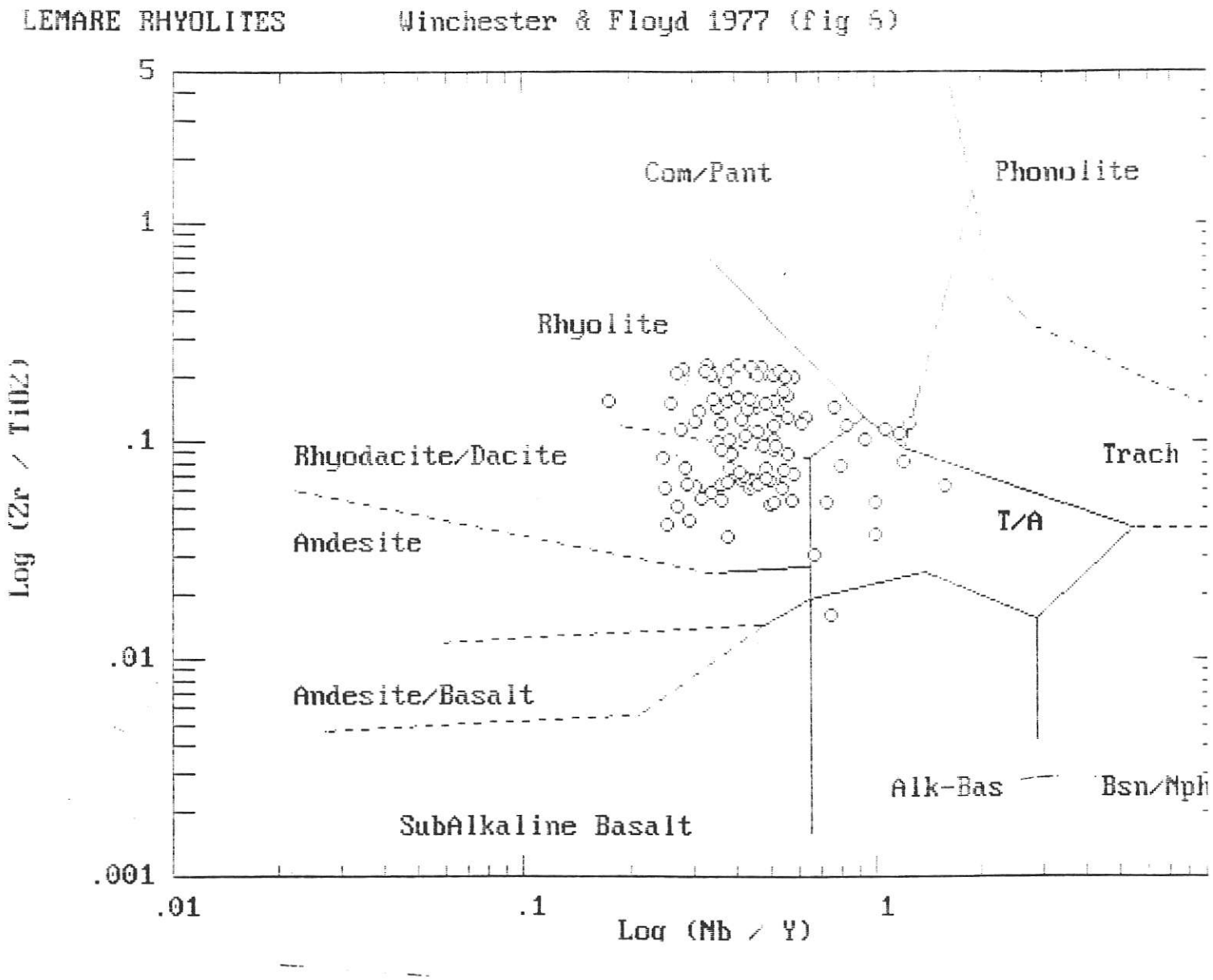

fig. 8 Discrimination plot for Lemare rhyolites

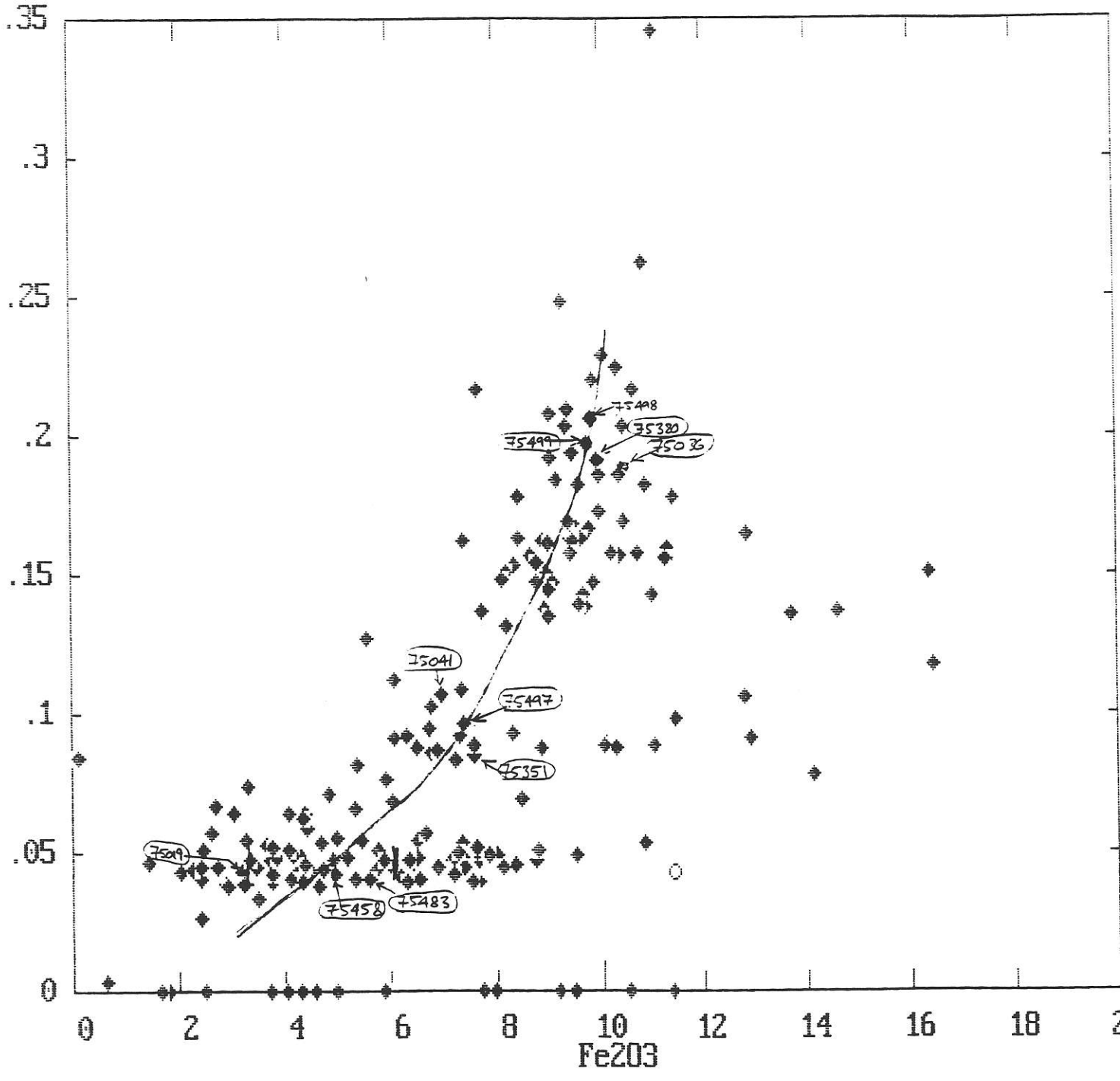

fig. 9 Fractionation trend : Fe2O3 vs. Al2O3/Zr

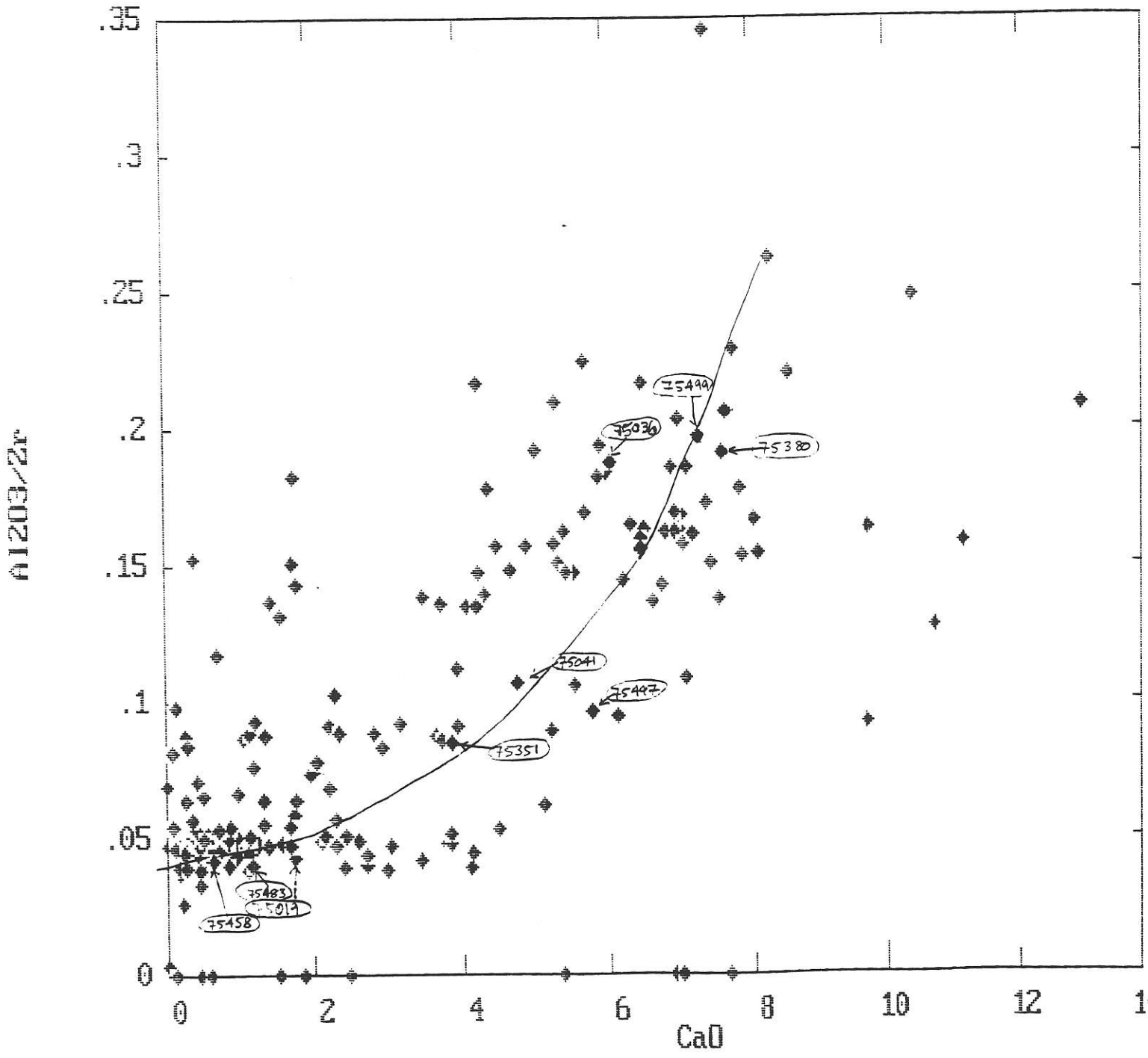

fig. 10 Fractionation trend : CaO vs. Al2O3/Zr

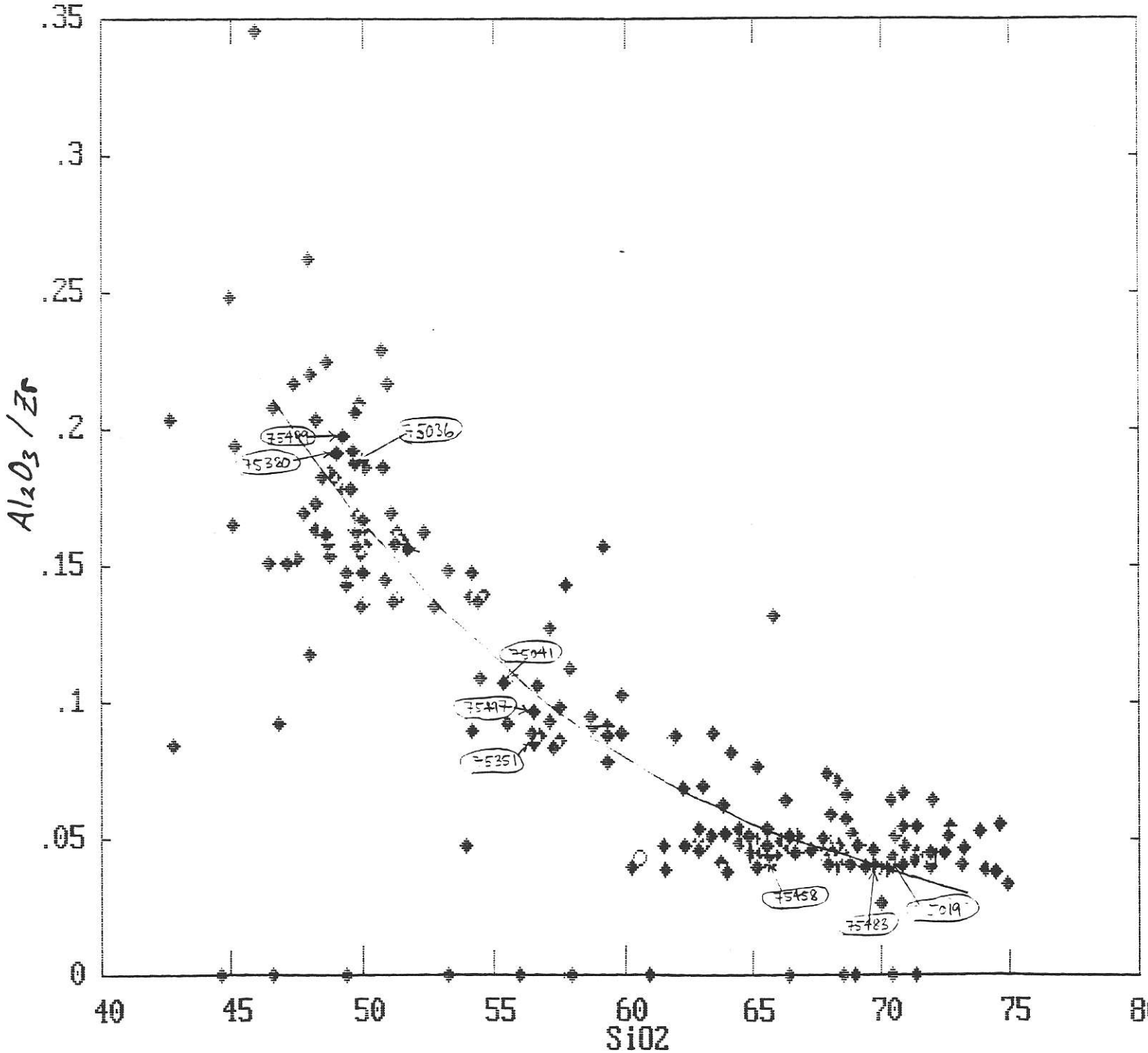

fig. 11 Fractionation trend : SiO2 vs. Al2O3/Zr

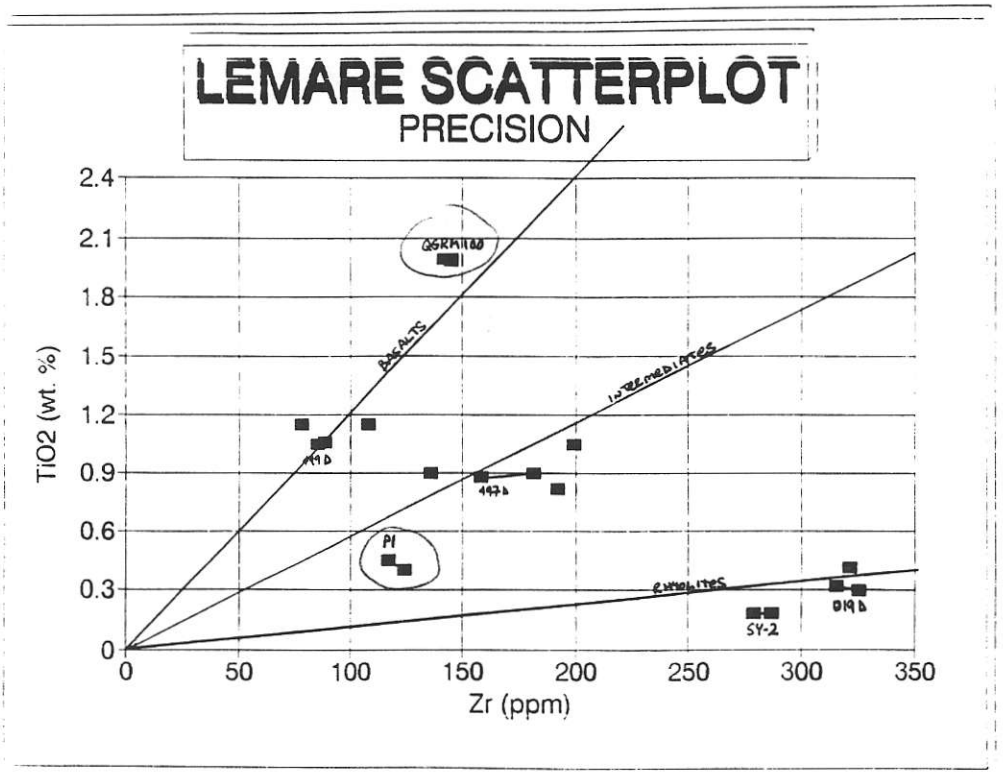

Fig. 12 Conserved Constituent and Duplicate Precision Scatterplot (All XRAL data).

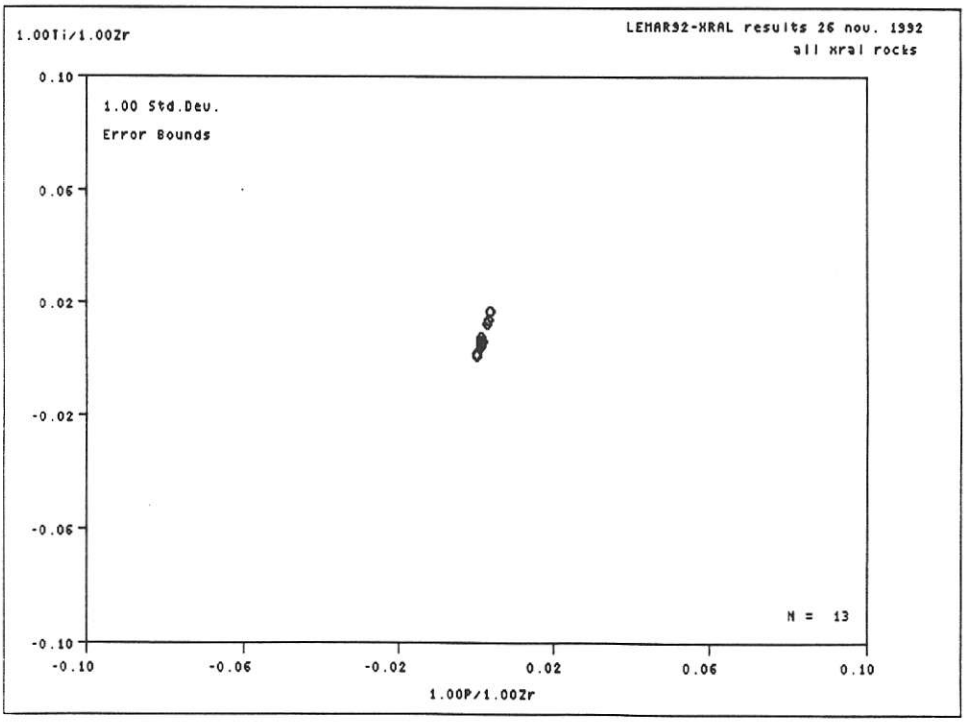

fig. 13 PER Diagram: Conserved Constituents (all XRAL data).

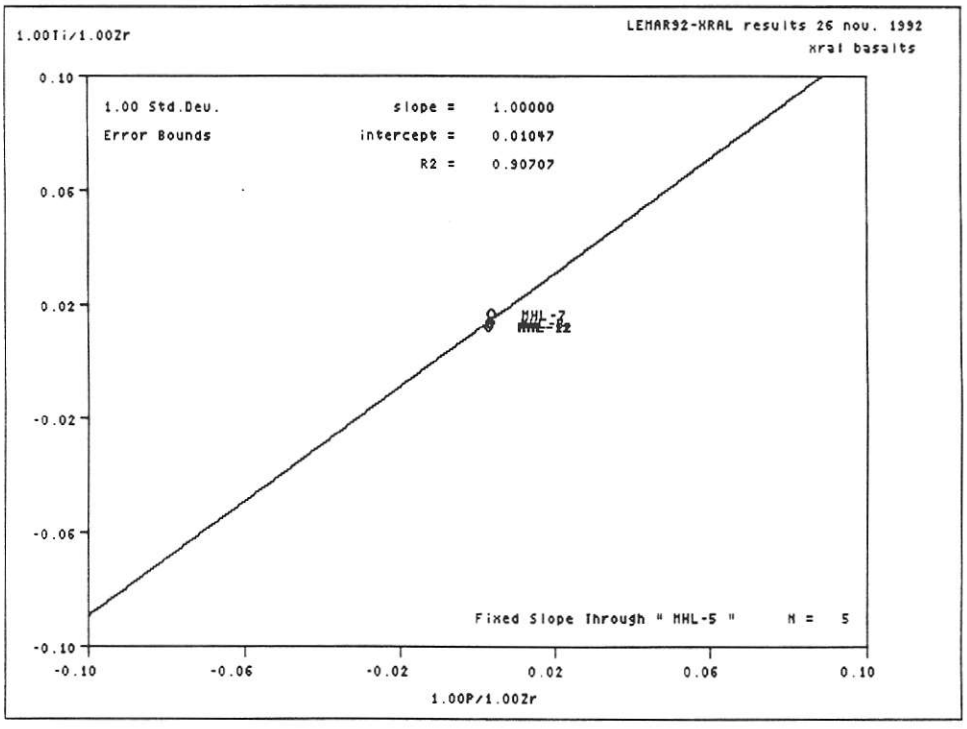

fig. 14 PER Diagram: Conserved Constituents (XRAL basalt data).

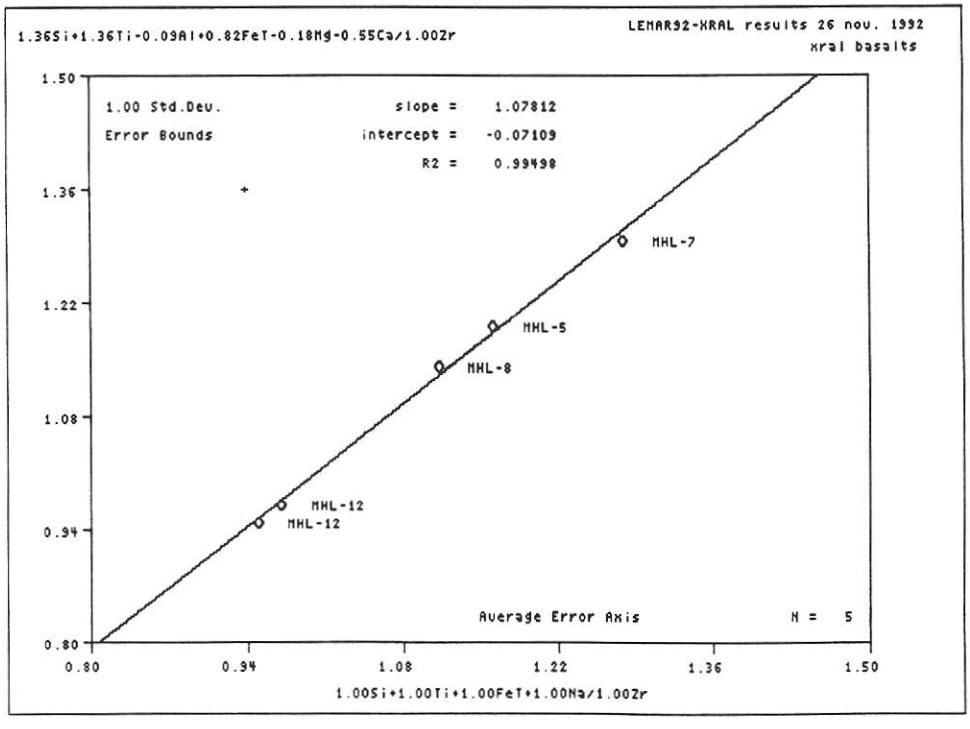

fig. 15 PER Diagram: 'Q PLOT' - Accounts for Plag, Ol, Pxy and Fe-oxide fractionation (XRAL basalts).

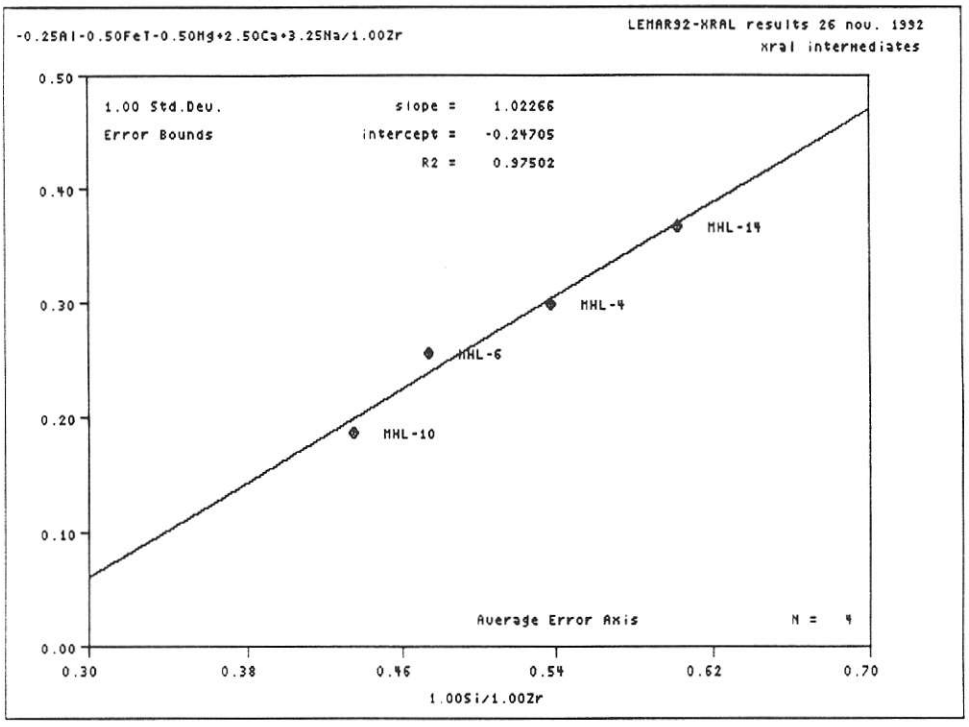

fig. 16 PER Diagram: Accounts for Plag and Pxy fractionation (XRAL intermediates).

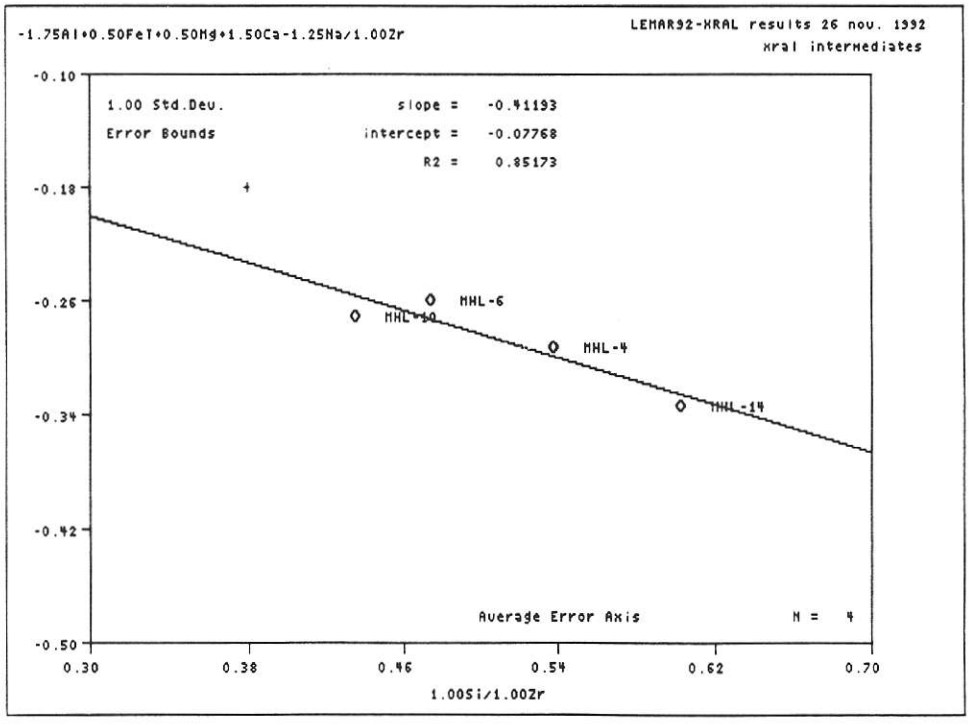

fig. 17 PER Diagram: Accounts for Ol and Pxy fractionation (XRAL intermediates).

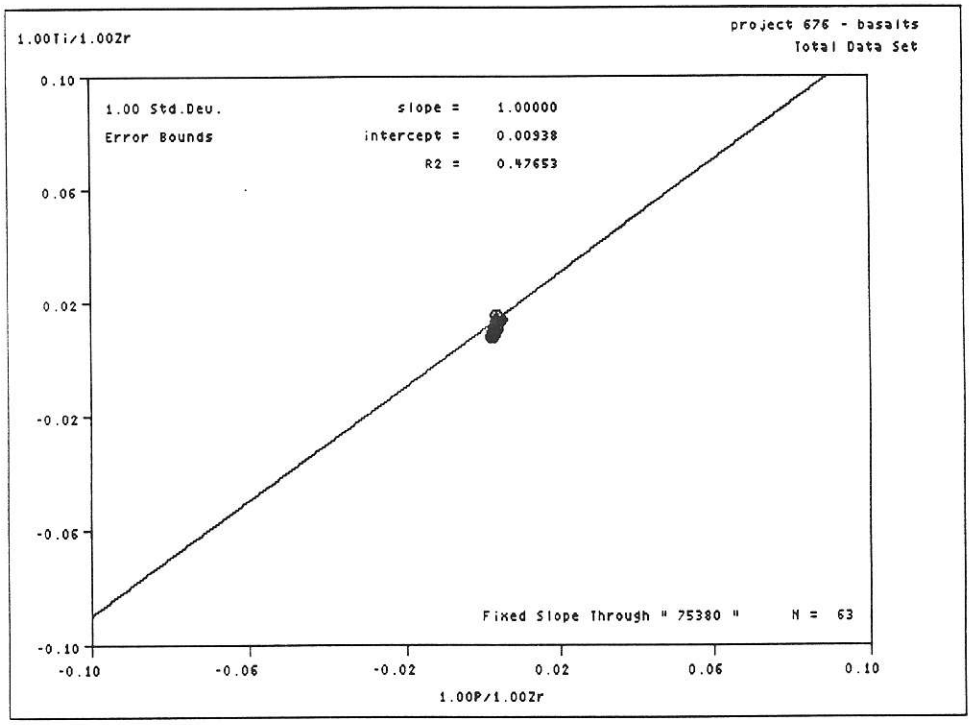

fig. 18 PER Diagram: Conserved Constituents (LEMARE basalts).

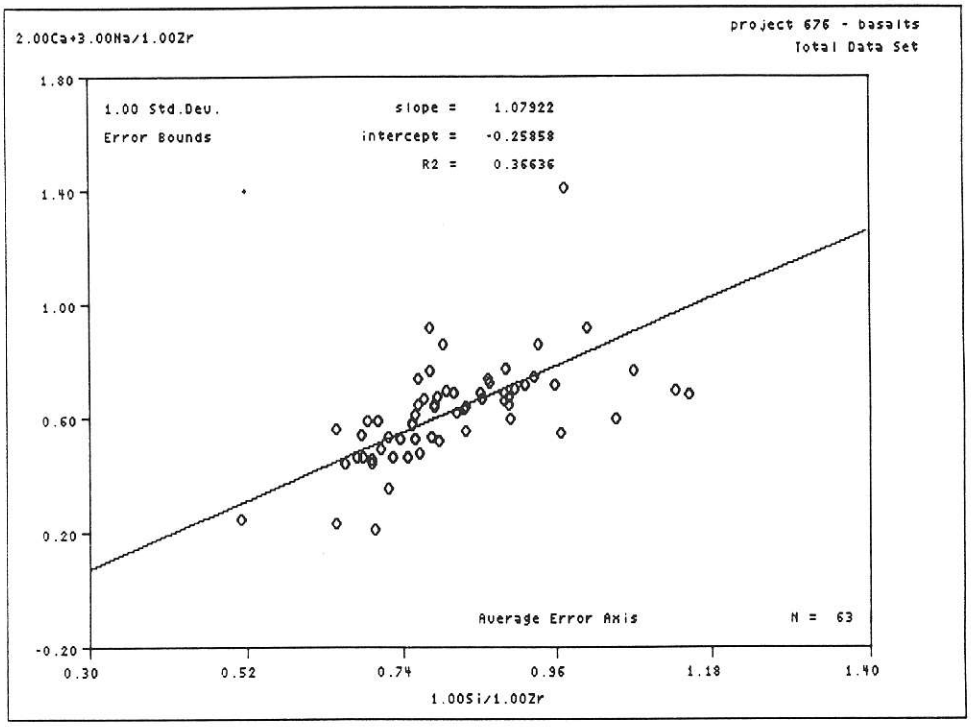

fig. 19 PER Diagram: Accounts for Plag fractionation - average error axis (LEMARE basalts).

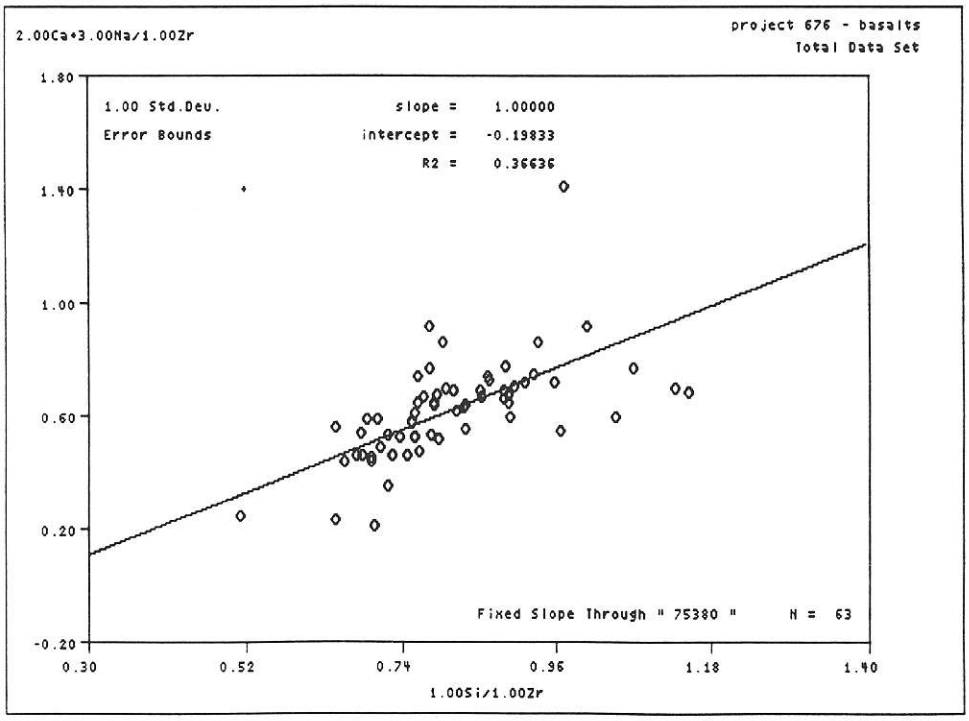

fig. 20 PER Diagram: Accounts for Plag fractionation - fixed slope axis [m=1] through 75380 (LEMARE basalts).

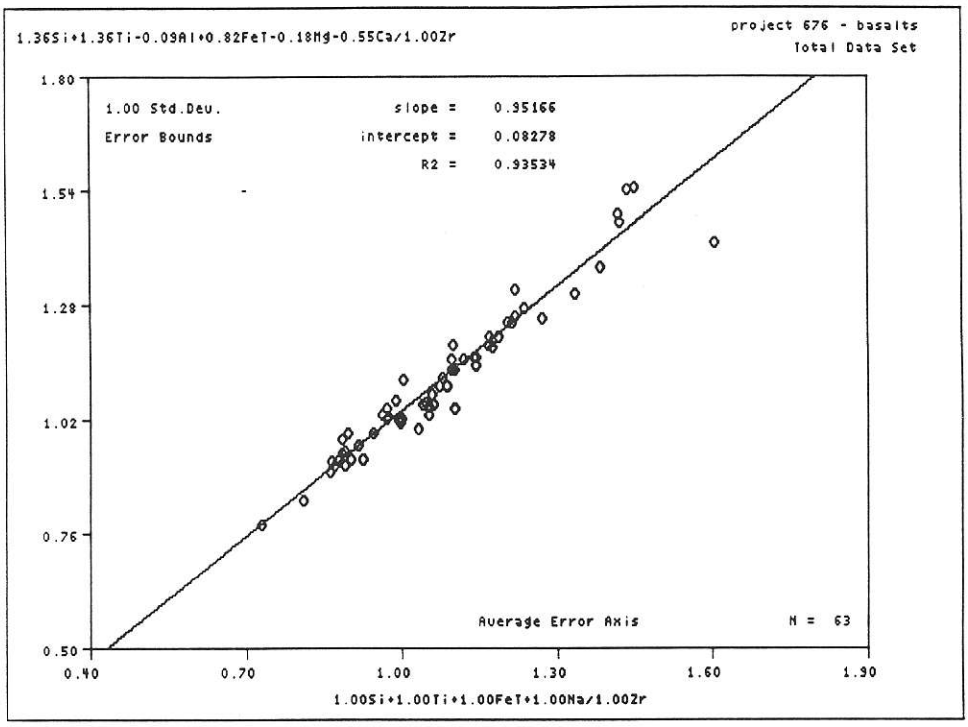

fig. 21 PER Diagram: 'Q PLOT' - average error axis (LEMARE basalts).

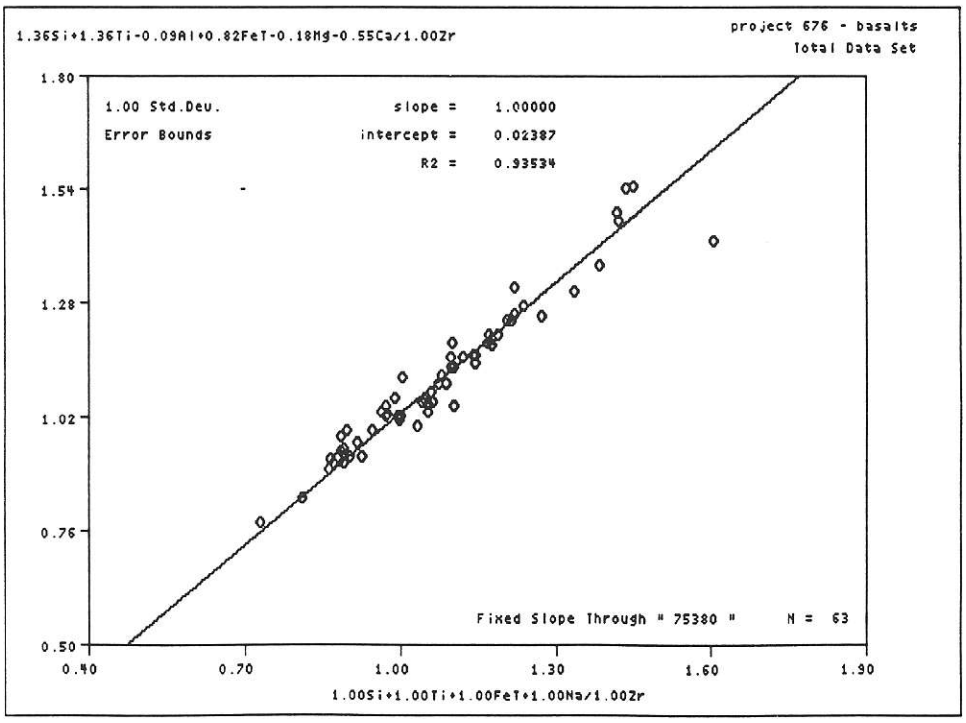

fig. 22 PER Diagram: 'Q PLOT' - fixed slope axis [m=1] through 75380 (LEMARE basalts).

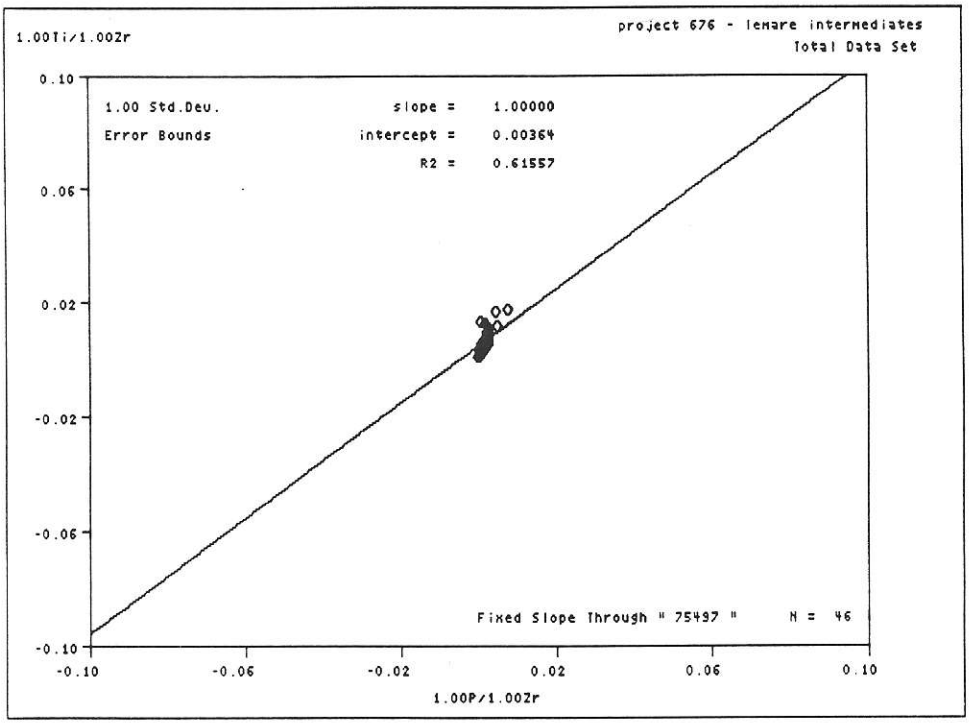

fig. 23 PER Diagram: Conserved Constituents (LEMARE intermediates).

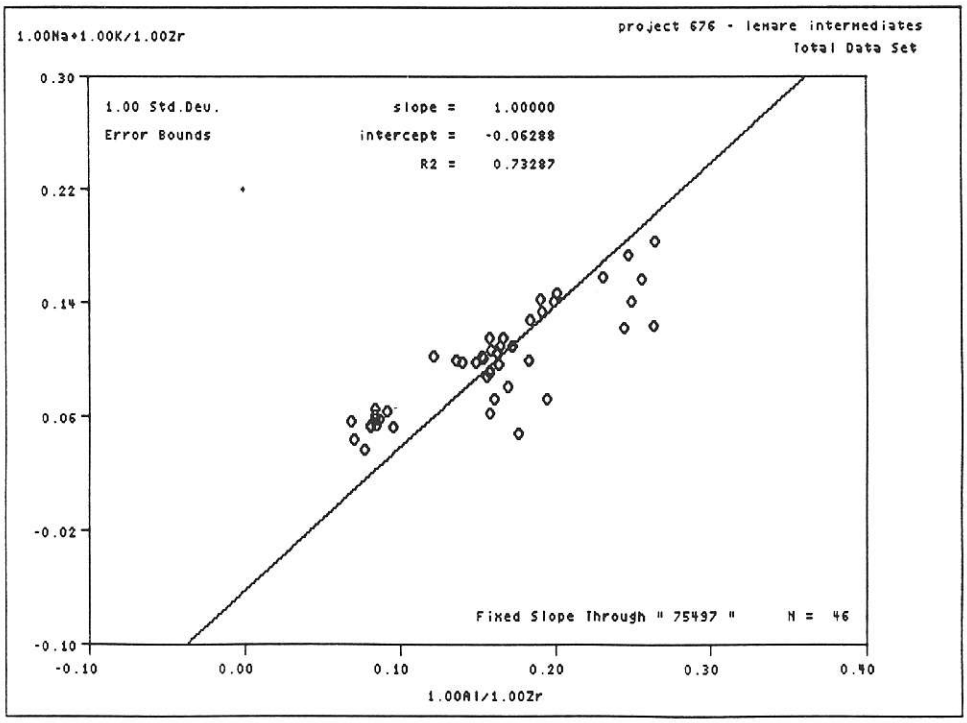

fig. 24 PER Diagram: Accounts for Alkali fractionation (LEMARE intermediates).

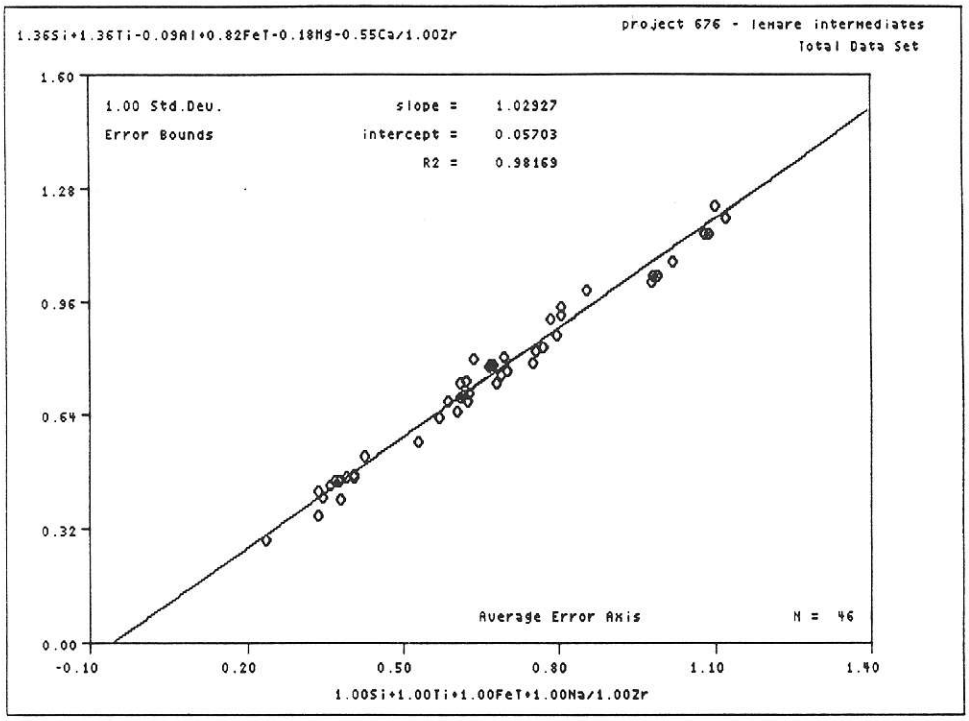

fig. 25 PER Diagram: 'Q PLOT' - average error axis (LEMARE intermediates).

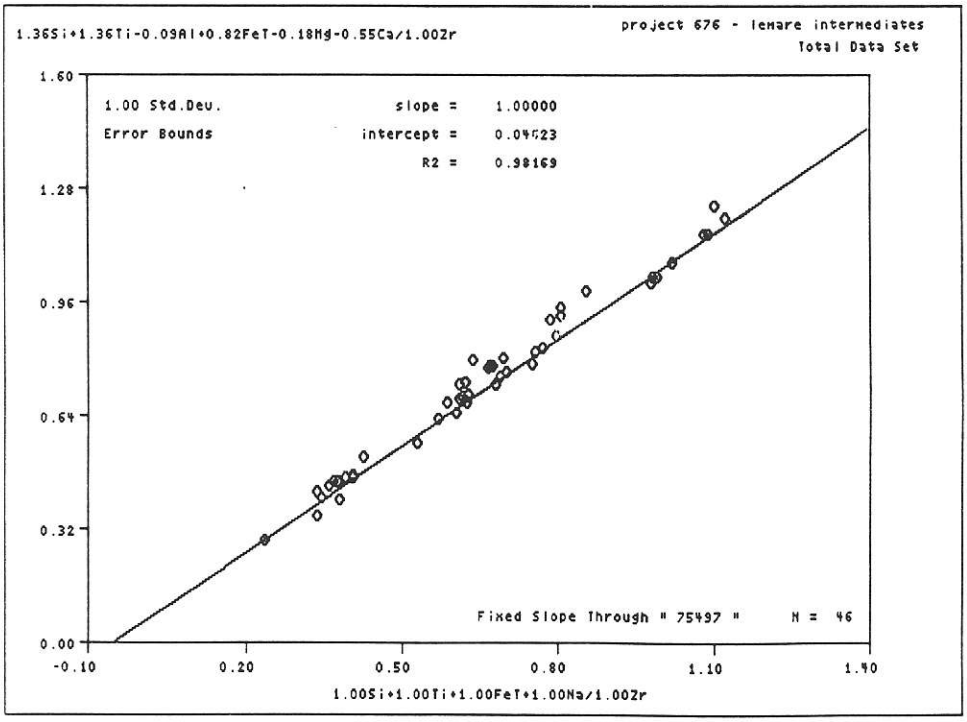

fig. 26 PER Diagram: 'Q PLOT' - fixed slope axis [m=1] through 75497 (LEMARE intermediates).

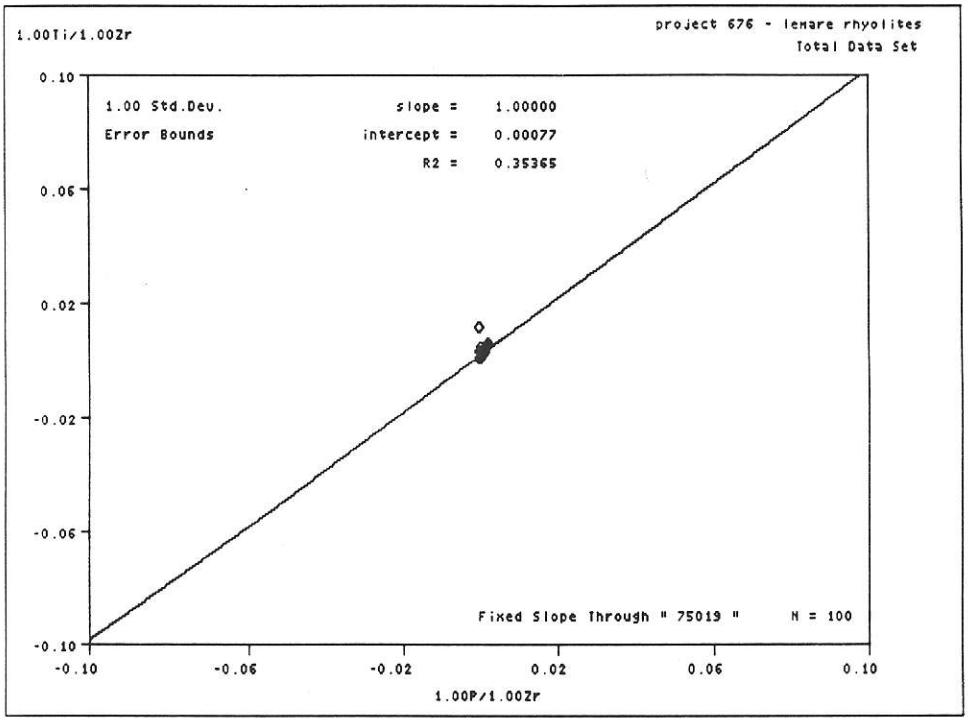

fig. 27 PER Diagram: Conserved Constituents (LEMARE rhyolites).

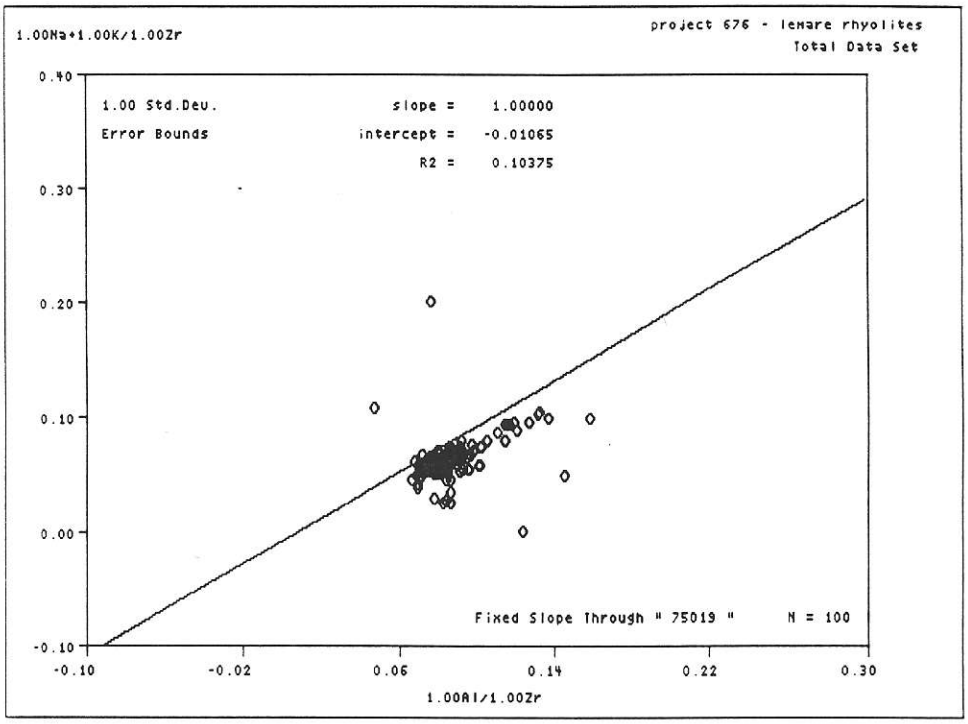

fig. 28 PER Diagram: Accounts for Alkali fractionation (LEMARE rhyolites).

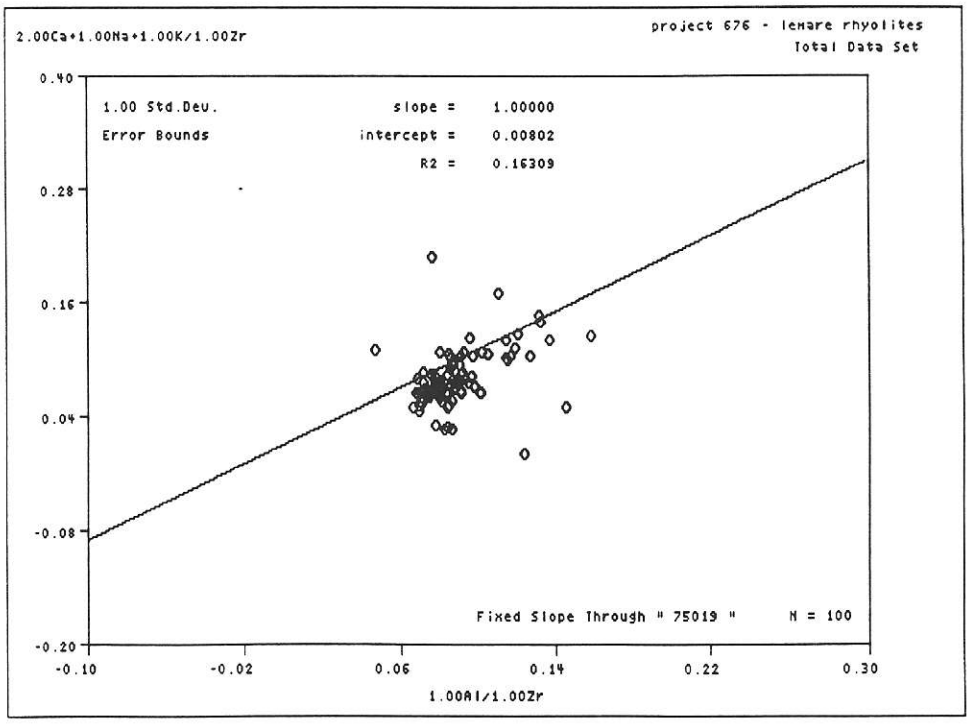

fig. 29 PER Diagram: Accounts for Felsic fractionation (LEMARE rhyolites).

PEARCE.PLOT ANALYSES FOR XRAL BASALTS				
PLOT	DENOMINATOR	SLOPE	INTERCEPT	CORR. COEF.
*CONS. CONST.	Zr	1.00	0.010	0.907
Q	Zr	1.08	-0.079	0.996
PLAG	Zr	0.686	0.088	0.920
PXY	Zr	0.654	0.041	0.996
OL	Zr	-0.244	0.913	0.559
PLAG+OL	Zr	0.644	-0.012	0.904
PLAG+PXY	Zr	0.729	0.188	0.933
PLAG+OL+PXY	Zr	0.331	-0.713	0.702
OL+PXY	Zr	0.163	0.010	0.996
PEARCE.PLOT ANALYSES FOR XRAL INTERMEDIATES				
Q	Zr	0.877	0.125	0.998
PLAG	Zr	1.25	-0.304	0.991
PXY	Zr	1.31	-0.444	0.911
OL	Zr	0.327	-0.111	0.911
PLAG+OL	Zr	1.54	-0.374	0.824
PLAG+PXY	Zr	1.02	0.213	0.986
PLAG+OL+PXY	Zr	1.55	-0.400	0.975
OL+PXY	Zr	-0.412	0.161	0.842
ALKALI	Zr	0.350	0.053	0.895
FELSIC	Zr	0.892	0.036	0.785
PEARCE.PLOT ANALYSES FOR XRAL RHYOLITES				
Q	Zr	1.32	-0.036	0.993
PLAG	Zr	-0.167	0.145	0.158
PXY	Zr	0.638	-0.186	0.908
OL	Zr	0.160	-0.047	0.908
PLAG+OL	Zr	0.457	0.018	0.997
PLAG+PXY	Zr	-0.378	0.200	0.390
PLAG+OL+PXY	Zr	0.042	0.090	0.019
OL+PXY	Zr	-0.047	-0.124	0.055
ALKALI	Zr	0.436	0.025	0.472
FELSIC	Zr	0.802	0.006	0.663

PEARCE.PLOT DATA FOR LEMARE BASALTS				
PLOT	~~NUMERATOR~~ DENOMINATOR	SLOPE	INTERCEPT	CORR. COEF.
*CONS. CONST.	Zr	1.00	0.009	0.477
Q	Zr	0.952	0.083	0.935
PLAG	Zr	1.08	-0.258	0.366
PXY	Zr	1.19	-0.458	0.587
OL	Zr	0.297	-0.114	0.587
PLAG+OL	Zr	0.921	-0.128	0.255
PLAG+PXY	Zr	0.922	-0.244	0.215
PLAG+OL+PXY	Zr	1.24	-0.272	0.523
OL+PXY	Zr	-0.454	-0.024	0.203
PEARCE.PLOT DATA FOR LEMARE INTERMEDIATES				
*CONS. CONST.	Zr	1.00	0.004	0.616
Q	Zr	1.03	0.057	0.982
PLAG	Zr	0.747	-0.145	0.648
PXY	Zr	0.644	-0.128	0.842
OL	Zr	0.161	-0.032	0.842
PLAG+OL	Zr	0.752	-0.017	0.751
PLAG+PXY	Zr	0.626	-0.133	0.515
PLAG+OL+PXY	Zr	0.903	-0.158	0.742
OL+PXY	Zr	-0.479	-0.006	0.655
*ALKALI	Zr	1.00	-0.063	0.733
FELSIC	Zr	1.33	-0.051	0.695
PEARCE.PLOT DATA FOR LEMARE RHYOLITES				
*CONS. CONST.	Zr	1.00	0.001	0.354
Q	Zr	1.11	0.039	0.931
PLAG	Zr	0.546	-0.103	0.175
PXY	Zr	0.242	-0.033	0.225
OL	Zr	0.061	-0.008	0.225
PLAG+OL	Zr	0.494	0.027	0.569
PLAG+PXY	Zr	0.497	0.110	0.123
PLAG+OL+PXY	Zr	0.594	-0.095	0.241
OL+PXY	Zr	-0.412	-0.007	0.440
*ALKALI	Zr	1.00	-0.027	0.104
FELSIC	Zr	1.33	-0.039	0.163

table 5----------Pearce.plot slope, intercept and correlation data